UCRL-19125

c.2

THE EFFECT OF ORDERING ON LATTICE HEAT CAPACITIES: ORDERED AND DISORDERED AuCu

Donald Thomson Hawkins

(Ph. D. Thesis)

March, 1970

UNIVERSITY OF CALIFORNIA

Lawrence Radiation Laboratory
Berkeley, California

AEC Contract No. W-7405-eng-48

2

DISCLAIMER

TABLE OF CONTENTS

LIST OF FIGURES

ABSTRACT

Heat capacities of pure gold and AuCu in both the ordered and disordered states have been measured between 20° and 298°K by isothermal calorimetry. Values for pure gold agree well with previous data except in the temperature range 70°- 150°K, where they are 0.5- 1.0% high. Combination of the heat capacity data for AuCu obtained in this study with existing high-temperature data yields the configurational entropy of the disordered state: $S^{\circ}_{0,\ \text{disordered}} = 1.280(\pm 0.1)$ e.u. This value is somewhat lower than the theoretical value of 1.38 e.u. expected for this alloy. The difference is attributed to short-range order, the existence of which is confirmed by heat of formation measurements. The effect of short-range ordering on the Cp values is discussed.

Ordered and disordered states both show a slight positive deviation from Kopp's Law up to about 175°K; then the deviations become slightly negative. The heat capacity of the disordered state is higher than that for the ordered state to 100°K, above which it becomes slightly lower. In agreement with previous data on $AuCu_3$ up to 4.2°K, little change of Cp on ordering was observed.

Details of the design and operation of the calorimeter are given.

I. INTRODUCTION

The scarcity of low-temperature heat capacity data on alloys is amazing. In the compilation by Hultgren, Orr, Anderson, and Kelley[1] in 1963, which presented data for 168 alloy systems, only 18 had any low-temperature data. Of these 18 systems, only 10 had data extending above 15°K. Since the orignial compilation appeared, revision of the systems with new or additional data has been proceeding, and to date 141 systems, many of which appeared in the 1963 compilation, have been evaluated.[2] Of these 141 systems, 63 have low-temperature Cp data, and 20 of these 63 have data above 15°K. While this shows a significant awareness of the need for such data, it is evident that far more work needs to be done in order to gain a clear understanding of the heat capacity of metallic alloys at low temperatures.

In 1819, Dulong and Petit[3] discovered that the heat capacity of solid elements at room temperature was about 6 cal/g-atom-degree. The failure of this law to hold at temperatures below room temperature was explained by Einstein[4] in 1907 with the application of quantum theory. Debye[5] later improved Einstein's model, assuming that the lattice vibrations covered not a single frequency but a broad spectrum of frequencies. Debye's result was that the lattice heat capacity is proportional to T^3 at low temperatures. This has been used extensively in extrapolating Cp curves to 0°K.

No measurements were made on the low-temperature Cp of alloys before 1930. Since that time, there has been a growing interest in this area, and at present there are many studies proceeding in the liquid helium range. These measurements are of interest in determining γ, the electronic contribution to Cp. The electronic heat capacity is proportional to the absolute temperature: $C_{el} = \gamma T$. C_{el} for alloys is of great interest in gaining an understanding of the density of states in the metallic state. Measurements of this type are one of the few direct methods of examining this phenomenon. A great deal of work is being done on the elements, but very little on alloys.

Even less work has been done on the lattice heat capacity of alloys. In 1864, Kopp[6] proposed that the heat capacity of a compound is equal to the sum of the heat capacities of the constituent elements. Kopp's Law, as this statement has come to be known, is widely used to estimate the heat capacities of alloys, although few experimental tests of its validity have been made. In many cases, Kopp's Law is assumed, whereas large deviations can exist, especially in the temperature range where Cp is rising rapidly. Lattice Cp values are of interest to the thermodynamicist in obtaining absolute entropies because the major contribution to S°_{298} occurs above 10°K. They are also of interest because the bond strength between the atoms can be at least qualitatively inferred from the lattice heat capacity. Since the Debye temperature, Θ_D, is directly proportional to the vibration frequency, a higher

Θ_D, or lower Cp, implies that a higher range of frequencies is effective, and hence a stronger bond. High-temperature thermodynamic data for alloys is fairly extensive, but could be made more complete if more low-temperature Cp data were available. Kopp's Law needs to be confirmed (or disproved) for alloys in general. In many cases, the zero point entropy, S°_0, is assumed to have the theoretical value for a random distribution of atoms, whereas considerable short-range order could be "frozen-in" at low temperatures.

No study has ever been made of the effect of ordering on the lattice heat capacity of an alloy.[7] Satterthwaite, Craig, and Wallace;[8] and Coffer, Craig, Krier, and Wallace[9] measured heat capacities of ordered Cd-Mg alloys but made no measurements on disordered samples. Such a study would be interesting because it would provide a means of calculating the zero point entropy of a "disordered" alloy (if high temperature entropy measurements were available), and short-range order should be detected by obtaining a value for S°_0 less than 1.38 e.u., the theoretical value of S°_0 for a random mixed 50-50 alloy. Eastman and Milner[10] investigated random solid solutions of AgCl and AgBr and obtained an entropy of formation at 0°K which agreed well with the value calculated from statistical considerations. No similar study on alloys has been made, although fully ordered samples can be prepared easily. Knowing S°_0 for such samples to be zero provides a ready check on the high-temperature data. The fact that the same sample,

given the proper heat treatment, can be prepared in either ordered or disordered state eliminates any uncertainties of composition between the two states. A further benefit of such measurements is that a test of Kopp's Law is provided.

The gold-copper system was chosen for this study because much previous work has already been done on this system.[1] High temperature heat and entropy of formation measurements at 800°K are available, as well as measurements of the heat of formation as a function of temperature from 298.15° to 900°K. These measurements can be used to calculate $\Delta S°$ at 298.15°K for the reaction:

$$Au_{0.5}Cu_{0.5(ordered)} = Au_{0.5}Cu_{0.5(disordered)}$$

All that is needed, therefore, to calculate the entropy at 0°K are measurements of Cp between 0° and 298.15°K for both ordered and disordered states.

Preparation and heat treatment of the sample is straightforward. According to Hansen,[11] AuCu melts over the range 889°- 893°C. The melting is nearly congruent, so that little segregation should occur on freezing. The structure of the disordered alloy is face-centered cubic with $a_0 = 3.847\text{Å}$,[12] and with copper and gold atoms randomly distributed. At 410°C, the alloy orders to an orthorhombic structure designated $AuCu^{II}$. This is a complex structure which can be looked on as 10 tetragonal unit cells placed side by side, with the copper and gold atoms arranged on alternate planes, reversing positions after

every five cells. The b/a ratio is 1.002, and the c/a ratio is 0.92. At about 385°C, $AuCu^{II}$ transforms to $AuCu^{I}$, which is tetragonal, with gold and copper atoms on alternate (002) planes, and with c/a = 0.93. The transformations are relatively rapid (they occur within a few hours at temperature) and reversible. Since the scattering powers of gold and copper differ significantly,[13] and additional superlattice lines are found, the three structures are readily detected by X-ray diffraction.

Although the alloys may appear to be completely disordered by X-ray studies, considerable short-range order can exist in the quenched specimens. Orr[14] has measured heats of formation of the ordered and disordered (quenched) alloys by liquid tin solution calorimetry. He found the heat of formation at 320°K of the ordered state to be -2150 cal/g-atom, and that of the disordered alloy to be -1630 cal/g-atom. In addition, Orr prepared the disordered alloy in the calorimeter and dropped it directly into the tin bath, finding ΔH to be -1230 cal/g-atom. The difference between the equilibrium state and the quenched state was attributed to the existence of short-range order. Heat of formation measurements provide a ready method of approximating the degree of short-range order in the sample used in the present measurements.

The method chosen for measuring the Cp of AuCu was isothermal calorimetry. A large part of the project centered around the redesign and rebuilding of an existing calorimeter, previously used by Huffstutler.[15]

The calorimeter will be described in considerable detail, so that this work can be used as an "operator's handbook" for future work with this apparatus. Isothermal calorimeters were first developed and used by Giauque and his coworkers;[16,17] the calorimeter used in this study was patterned after Giauque's design. Briefly, it consists of a specimen container around which is wound a coil of wire. The wire serves both as a heater and resistance thermometer. The container is surrounded by a heavy jacket maintained in a vacuum during measurements, and the vacuum system is submerged in a liquefied gas to maintain a low temperature. From measurements of the energy input, determined from the heater voltage and current, and the temperature rise, as measured with the resistance thermometer, the heat capacity is determined. Corrections for heat leak and Newton's Law heat transfer must be made. Complete details of the apparatus are given in the following section. An excellent review of the method of isothermal calorimetry is given by Stout.[18]

II. EXPERIMENTAL APPARATUS

Preliminary measurements on copper using Huffstutler's apparatus[15] proved to have 2-3% scatter, particularly above 200°K. In this region, drift rate measurements became difficult due to unstable galvanometer readings. The gold foil covering the calorimeter can had begun to flake off, exposing the bakelite insulation. It also became increasingly difficult to maintain a steady vacuum in the system. For these reasons, the apparatus was completely disassembled and reconstructed. A new calorimeter can was machined, and the vacuum system was redesigned to eliminate as many right-angle bends and "dead spots" as possible. A flexible liquid gas transfer line eliminated the need of hoisting the hydrogen supply dewar and raising and lowering the transfer line, thus gaining a considerable measure of safety. The following paragraphs describe in detail the redesigned apparatus.

The Calorimeter Assembly

The calorimeter can, shown in Figure 1, was machined from copper tubing. It is $5\frac{1}{4}$ inches long, $1\frac{1}{2}$ inches in diameter, with 0.015 inch wall thickness. The bottom has thickness 0.030 inch. The top "chimney" is machined from Monel to 0.030 inch thickness. Volume of the can, including "chimney", is 154 cm^3. All joints were silver soldered, then tinned over with soft solder. The top, $\frac{1}{2}$ inch in diameter, is soldered in place with 60/40 soft solder after insertion

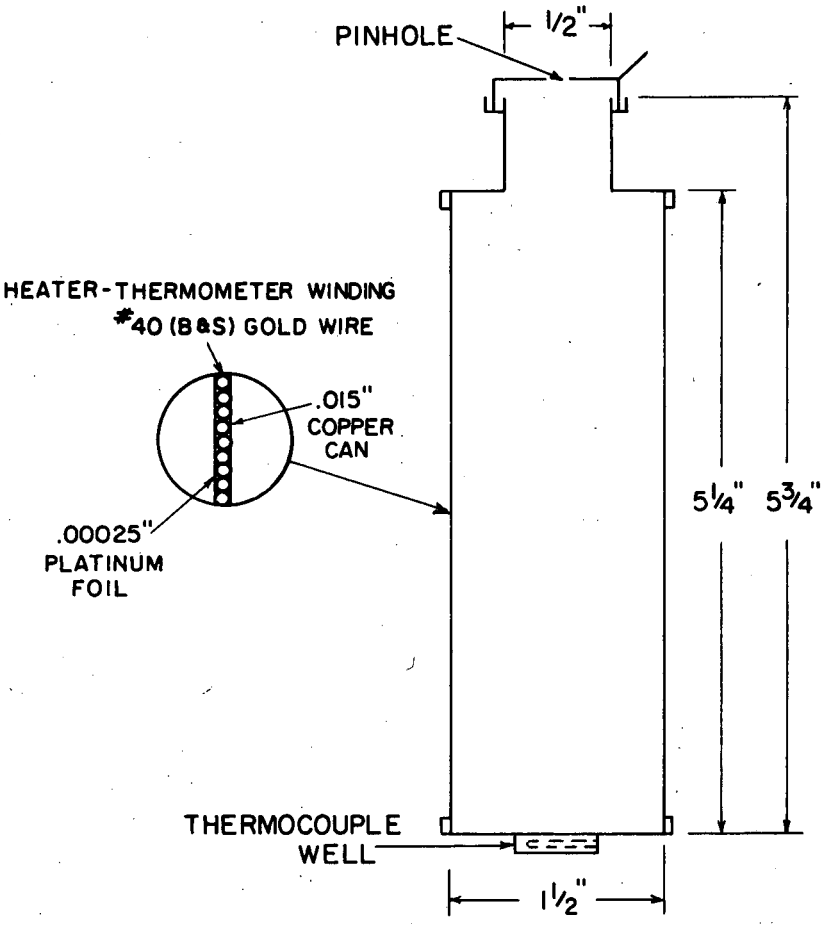

FIGURE 1. CALORIMETER CAN AND TOP.

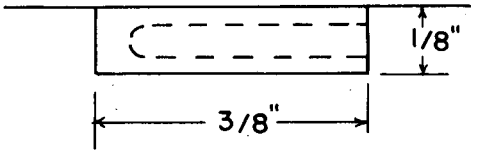

FIGURE 1a. DETAIL OF THERMOCOUPLE WELL.

XBL 6912-6632

of the sample. A pinhole in the top is closed after placing the assembled calorimeter can in a vacuum desiccator, pumping out the air, flushing, and backfilling with about 1 atm of helium. On the bottom of the can is soldered a small well into which the calibrated copper-constantan thermocouple is inserted.

After leak testing and thorough cleaning, the surface of the can was lightly rubbed with 4/0 emery paper, rinsed in alcohol, and coated with 3 light coats of GE 7031 Formvar varnish. This varnish, after baking under a heat lamp for 45 minutes between coats and then in an oven at 125°C for $2\frac{1}{2}$ hours after all 3 coats were applied, provides electrical insulation between the can and the heater winding.

After coating, the can was wrapped in a towel, placed in a large diameter glass tube, slowly cooled to liquid air temperature, and then slowly warmed. This procedure was repeated several times. Liquid air rather than liquid nitrogen was used because liquid nitrogen would condense liquid oxygen from the air, which, in contact with the cotton towel, would create a possible fire hazard, as well as cool the can too rapidly. The purpose of this procedure is to remove strains in the varnish before winding the thermometer-heater.

The calorimeter heater-resistance thermometer consists of 612 turns of No. 40 (B and S) silk-wrapped gold wire tightly wound over the length of the can. The ends of the gold wire were soldered to 0.002 inch thick, 1/16 inch wide strips of copper foil wrapped around

the ends of the can and insulated from it by strips of mica placed between the can and the foil. Measured resistance at room temperature agreed well with that calculated from the resistivity of No. 40 gold wire and the known length (7325 cm) of wire in the winding. The resistance of the thermometer varies from about 18 ohms at 15°K to about 340 ohms at room temperature.

Three more light coats of GE 7031 varnish were applied; the varnish was air dried between coats. The outer surface of the winding was covered with 0.0025 inch platinum foil, held in place by the final coat of varnish. The entire assembled calorimeter was baked at 55°C for 2 hours, then at 125°C for a further 2 hours.

The calorimeter is surrounded by a heavy copper jacket, as shown in Figure 2. The jacket is wound with No. 32 (B and S) Formvar insulated manganin resistance wire. Manganin was chosen because of its low temperature coefficient of resistance. The resistance of the jacket heater is about 320 ohms. The lower, removable section of the jacket is held firmly to the top by three bolts. A large (2500 gm) mass of lead was cast into the top of the jacket to raise the total Cp of the system at low temperatures providing good thermal inertia. The inner surface of the lower part of the jacket, which is exposed to the calorimeter, was gold plated to make the surface emissivities of the jacket and calorimeter as nearly equal as possible. The jacket is suspended from the top of the outer can by three linen cords, thus

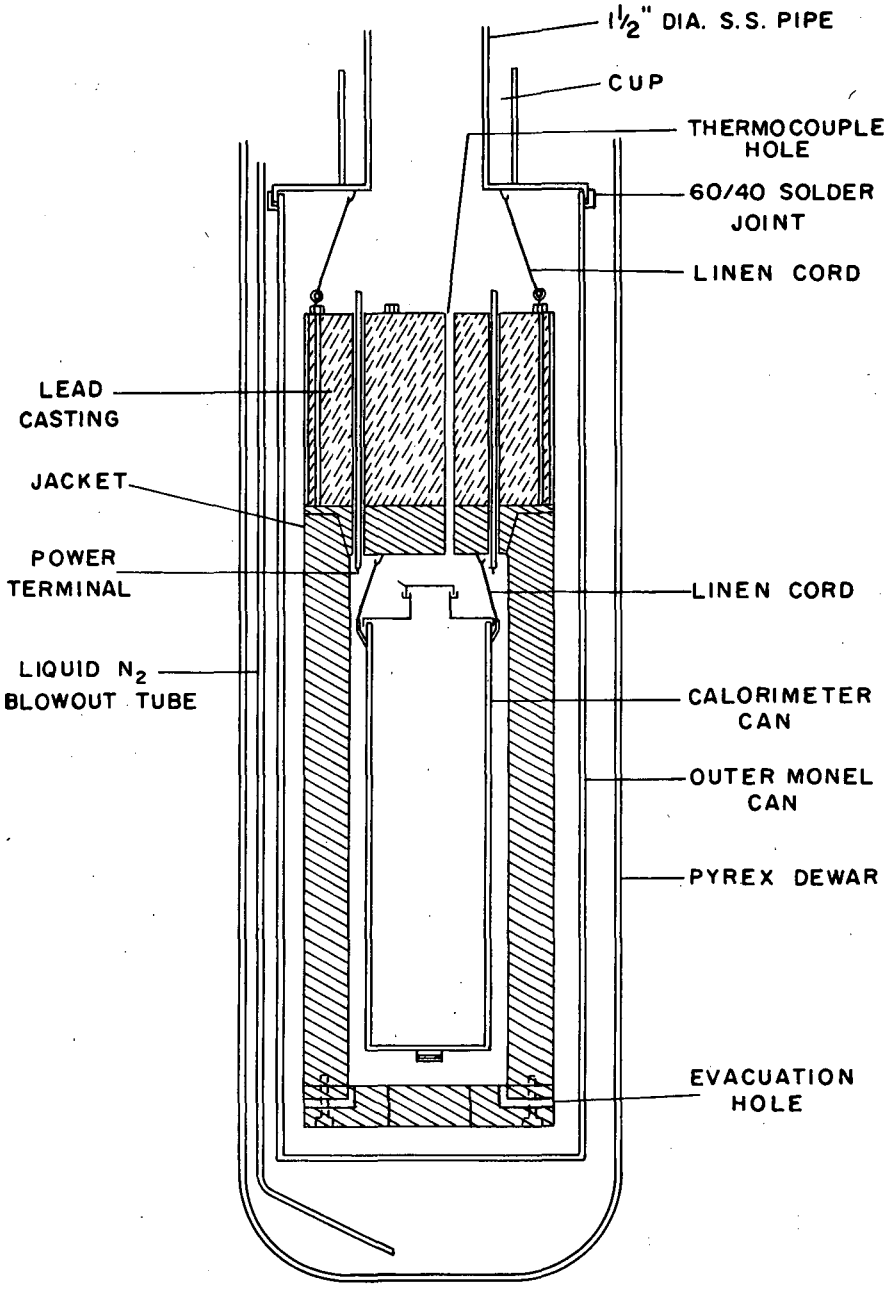

FIGURE 2. CALORIMETER CAN AND JACKET ASSEMBLY. (HIGH-VACUUM SYSTEM)

XBL 6912-6631

providing minimum thermal contact for the calorimeter. The calorimeter can is suspended by linen cords from the bottom of the upper part of the jacket. Six holes near the bottom of the jacket provide for its rapid evacuation. Hardwood plugs loosely inserted into three of these holes serve to center the jacket in the outer can.

The entire jacket-calorimeter assembly is surrounded by a Monel can soft soldered with 60/40 solder to the top support plate. A "cup" on the outside of the plate is filled with water during soldering operations to prevent overheating of the plate and stainless steel tube and thus damaging the insulation on the wires inside.

Power leads are brought through a stainless steel pipe $1\frac{1}{2}$ inches in diameter and connected to Formvar insulated copper lugs which extend through the top portion of the jeacket. The lugs are held in place with Wood's Metal. Connections to the calorimeter winding are made with No. 40 (B and S) copper leads.

Thermocouples, insulated with fiberglass sleeving, are wound around the top portion of the jacket to reduce any immersion error, then passed through a hole in the top of the jacket. This hole was filled with paraffin after insertion of the wires so as to reduce the heat leak. The copper-constantan jacket thermocouple is bolted to the lower surface of the jacket top. The 4-strand [3 No. 30 (B and S) constantan wires and 1 No. 30 copper wire] calibrated calorimeter thermocouple is sewn to a $\frac{1}{4}$ inch wide, 23 inches long cotton tape and

wound around the calorimeter can several times before being inserted into the well provided for it. Wood's Metal holds the junction securely in place as well as insuring good thermal contact. The thermocouple wires are tied tightly to the outer surface of the can with silk thread to prevent them from coming into contact with the lower portion of the jacket. Figure 2a is a photograph of the high vacuum system as assembled with the lower portion of the jacket removed.

The High Vacuum System

Lead wires down the stainless steel pipe are Formvar insulated. Jacket heater leads are No. 24 (B and S); all other wires are No. 30 (B and S). Several extra wires were installed for future use if needed. Wires were brought out of the system through a Kovar seal soldered into place directly above the calorimeter-jacket assembly. Thermocouple wires were sealed into place with de Khotinsky cement; all other wires were soft soldered. The general arrangement of the vacuum system is shown in Figure 3.

The stainless steel $1\frac{1}{2}$ inch diameter pipe is connected directly to the $1\frac{1}{2}$ inch diameter vacuum manifold. For safety reasons the vacuum pumps are located on the floor, below the calorimeter, and 8 feet away. The Philips Type PHG-09 vacuum gauge tube is located about 3 feet from the top of the stainless steel pipe, and is sealed in place by means of a Sealastic fitting. A high-speed (800 liters/sec) NRC HS 700 diffusion pump is backed by a 3.2 cfm NRC type 4D mechanical pump.

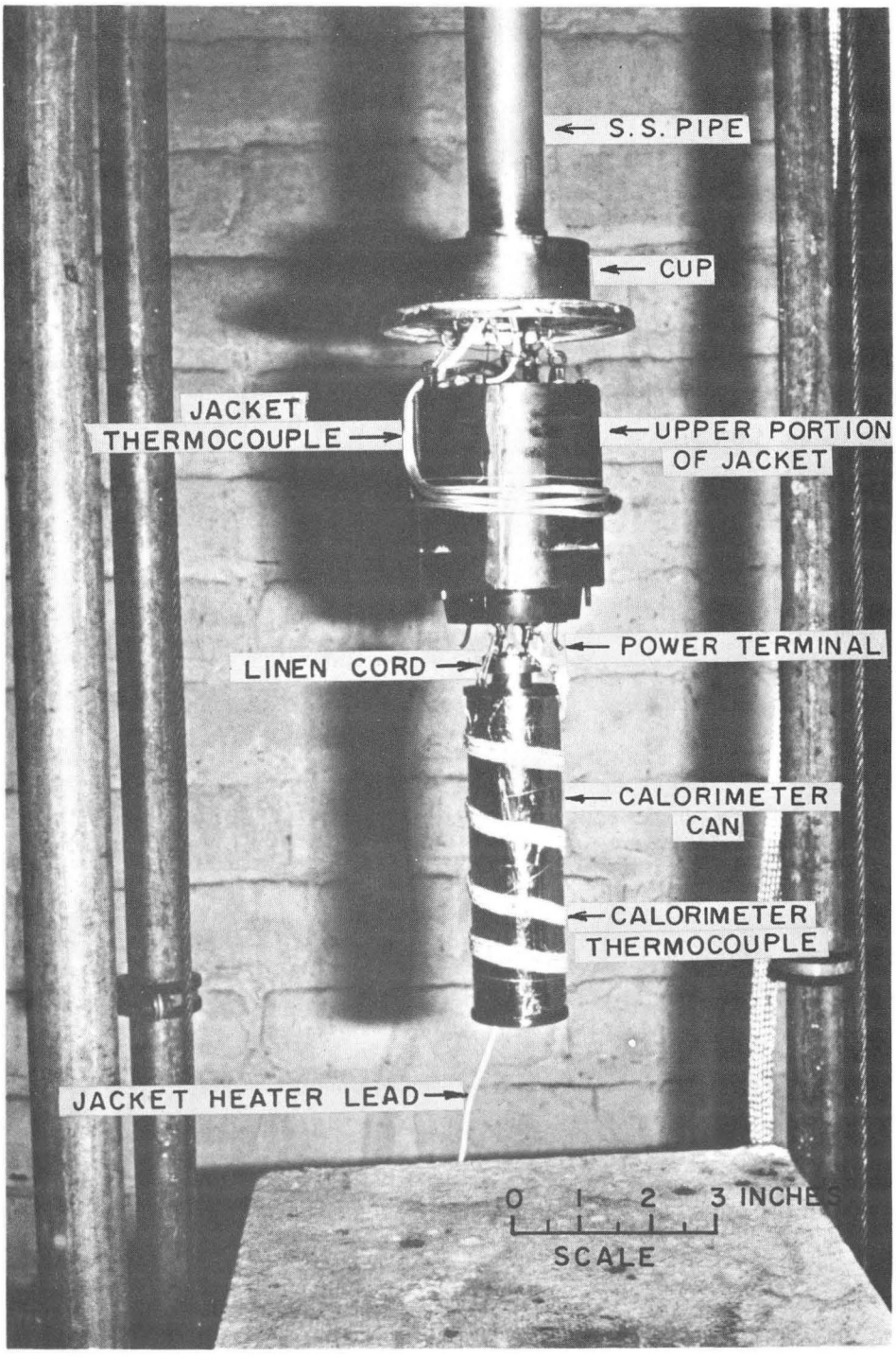

Figure 2a. View of Calorimeter and Upper Portion of Jacket, as assembled.

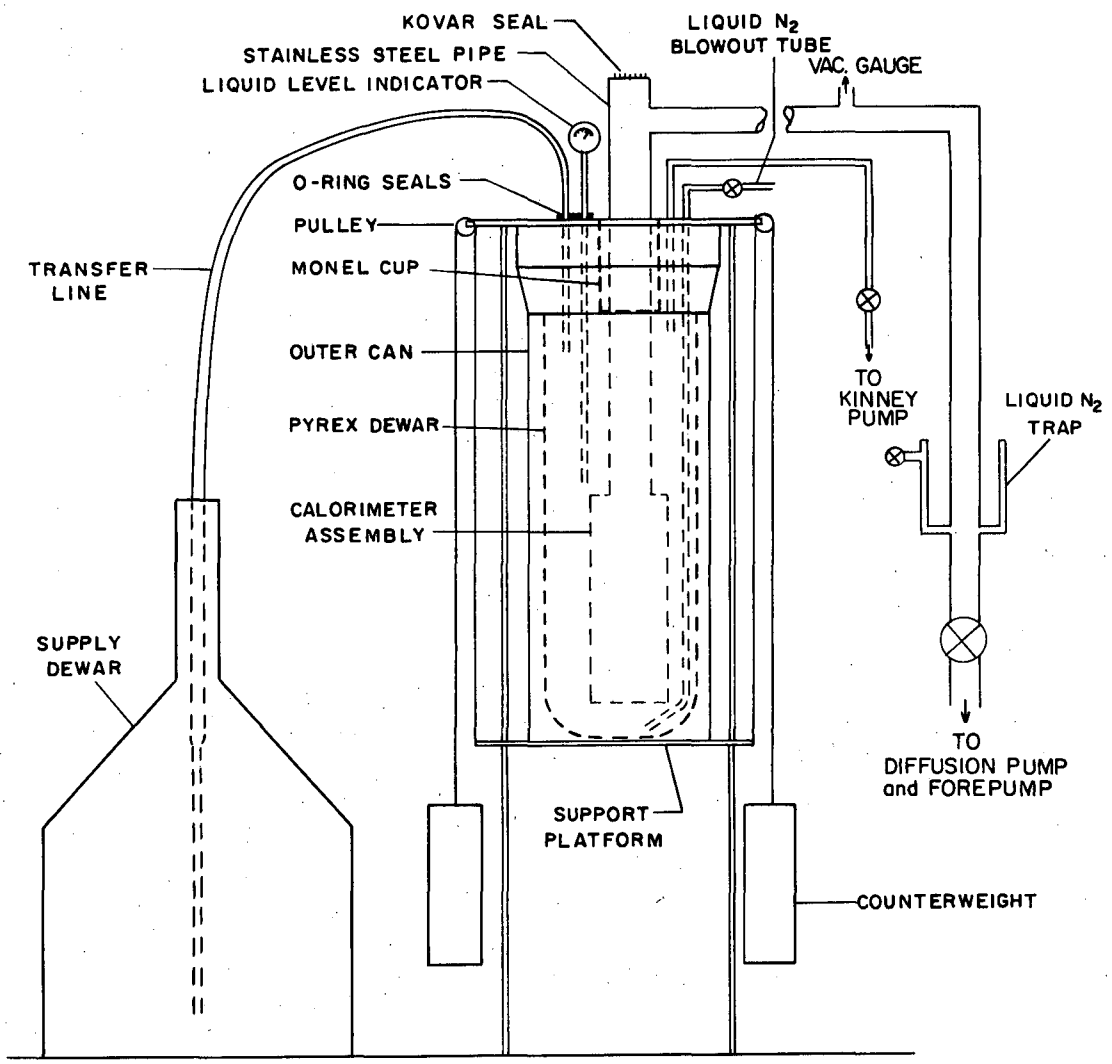

FIGURE 3 GENERAL ARRANGEMENT OF APPARATUS.

XBL 6912-6633

The pumps are connected to the manifold through a 1 inch diameter flange-type gate valve.* A stainless steel liquid nitrogen trap protects the system from contamination by vacuum pump oil vapors. Before installation of the calorimeter assembly, the system was leak tested and found to be capable of a vacuum of 3×10^{-7} torr after pumping for 48 hours. In use, pressures were about 8×10^{-6} torr at room temperature and less than 10^{-7} torr at liquid nitrogen temperatures. Despite the long manifold, pressures remained constant at constant temperature. Heat leaks, as evidenced by temperature drift rates, remained small, even at liquid hydrogen temperatures.

The Low-Vacuum System

The low-vacuum system, also shown in Figure 3, provides a closed system for control of exhaust gases from liquid nitrogen and liquid hydrogen, as well as preventing air from condensing in the system and creating an explosion hazard. It also provides a means of pumping on the cryogenic liquid to reduce its boiling point.

The stainless steel pipe containing the lead wires and forming part of the high-vacuum system is welded into a steel plate supported by a stand rigidly bolted to the floor. Openings in this plate admit the transfer line, exhaust line, vacuum line, liquid level indicator, and liquid nitrogen blowout tube. All tubes and pipes entering the low-vacuum system are made of stainless steel to reduce heat leak. In addition,

*Vacuum Research Company, San Leandro, California

a Monel cup about 6 inches long surrounding the stainless steel high-vacuum pipe is kept full of a dry ice-acetone bath during measurements, in order to further reduce heat leak.

The liquid gas transfer line is flexible, bellows type, and vacuum jacketed,* especially made for efficient transfer of cryogenic liquids. It is sealed into place by means of a Sealastic fitting. A sliding "pressure hat" quickly and easily adapts to any size supply dewar and provides a connection to a helium cylinder for pressurization of the supply dewar. Use of a flexible transfer line eliminated the need for raising the supply dewars on a hoisting platform as was done by Huffstutler. Huffstutler's transfer line was rigid and had to be raised and lowered through an O-ring seal to accommodate the different sized dewars used to transport liquid nitrogen and liquid hydrogen. This was a risky operation, at best, when using liquid hydrogen.

The exhaust line (not shown in Figure 3) is made of 1 inch diameter copper pipe. A pressure relief valve consisting of a stainless steel plate resting on an O-ring maintains a constant pressure of 2 psi on the system. Higher pressures, needed when blowing out liquid nitrogen prior to introducing liquid hydrogen, can be obtained by means of a lever held down on the stainless steel plate. A safety pressure release valve is set for 10 psi and would provide additional venting of the system in case of a large or sudden heat leak which would occur, for instance,

*Janis Research Company, Stoneham, Massachussetts, Model FHT.

by failure of the high vacuum system.

The liquid level indicator, made by the Lawrence Radiation Laboratory mechanical shops, measures the pressure differential between the upper and lower end of the gauge tube. The gauge is calibrated in inches of liquid hydrogen. It provides a ready check on the rate of consumption of liquid hydrogen and also gives an indication of when the dewar is full. The liquid level indicator is sealed into place with a Sealastic-type fitting using a teflon O-ring.

The liquid nitrogen blowout tube is a 3/16 inch diameter thin wall stainless tube soldered into the upper plate. It is closed off by a needle valve.

The low-vacuum system is evacuated through a 1 inch diameter copper pipe by a Kinney Model KS-13 pump, which is capable of rapid pumping of large volumes of gas.

A Pyrex dewar inside a stainless steel can holds the cryogenic liquid. The can and dewar rest on a moveable platform, counterbalanced by lead weights. This arrangement allows the dewar to be raised so that the cyrogenic liquid surrounds the high-vacuum can as well as about 20 inches of the support pipe. The can is held in place by 16 bolts which are carefully tightened with a torque wrench. A carefully machined ball-vee flange joint similar to that used by Giauque[16,17] gives a good seal.

One might think that, with liquid helium readily available and thus

with the possibility of making measurements to or below 4.2°K, considerable risk could be eliminated and considerable advantage gained by using liquid helium instead of liquid hydrogen to attain low temperatures. A variety of reasons prevent this. Resistance thermometers suitable at liquid helium temperatures may not be usable at higher temperatures, and vice versa. A very considerable amount of helium would be needed because the heat of vaporization of liquid helium is much less than that of liquid hydrogen,[19] thus requiring a prohibitive amount of the liquid to remove the heat in the sample below 20°K. (Calorimeters operating in the liquid helium temperature range have heat exchangers so that the temperature is lowered by contact with the cold gas as well as by the vaporization of helium.) It is doubtful whether stable temperatures in the liquid helium range could be obtained with the present apparatus. Finally, for the purposes of this study, i.e., obtaining entropies at 298°K, the extrapolation below 20°K is small and does not introduce a significant uncertainty.

Electrical Circuitry

Electrical measurements were made on a White double potentiometer, using an ultrasensitive galvanometer with an optical lever system.* Voltages could be easily read to the nearest 0.1 microvolt.

The electrical circuits are shown in Figure 4. (Numbers refer to switch positions.) Power was supplied to the calorimeter heater by

*Leeds and Northrup Company, Philadelphia, Pennsylvania

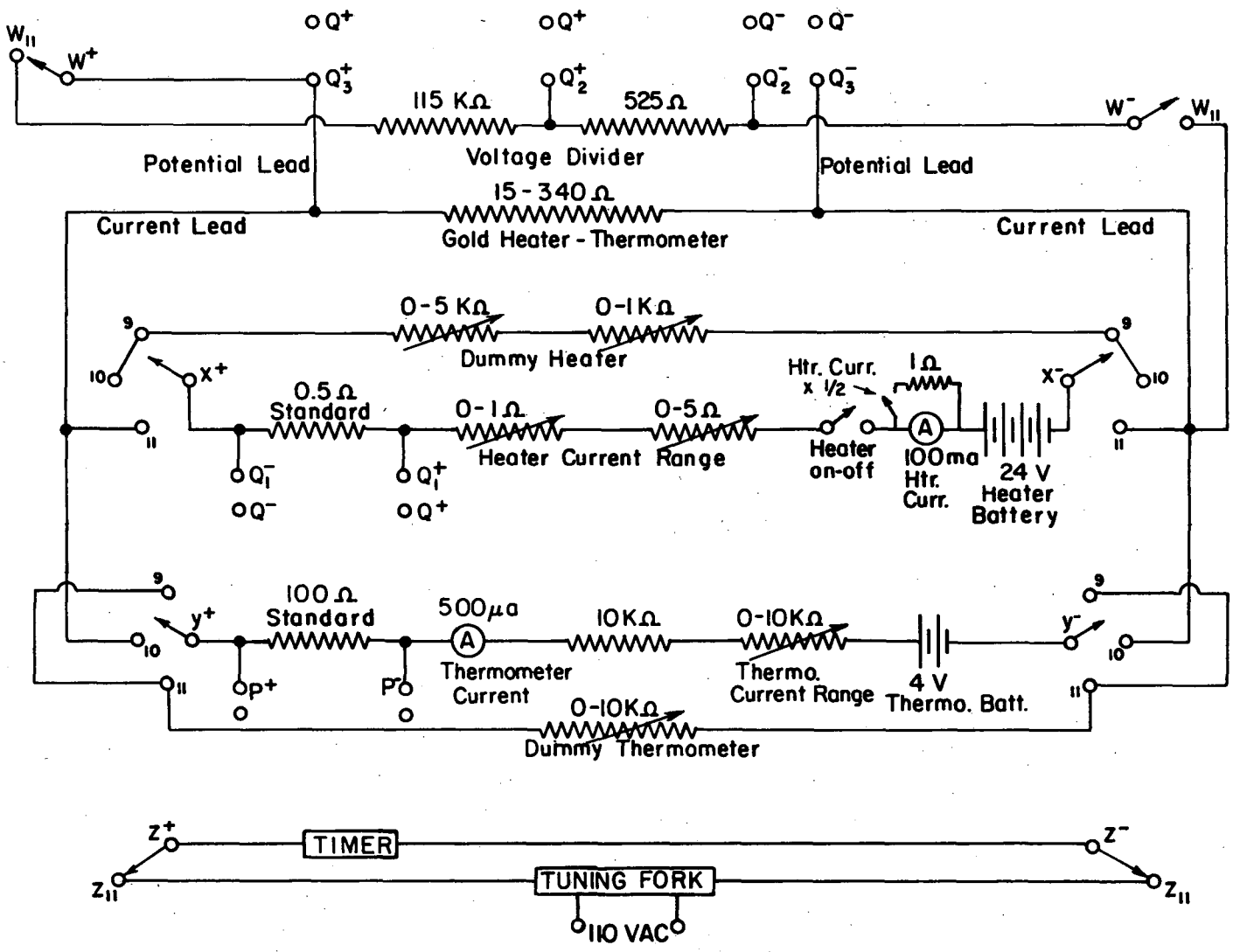

FIGURE 4. CIRCUIT DIAGRAM.

XBL 6912-6634

means of two heavy-duty (100 ampere-hour) 12 volt storage batteries. All batteries were placed in a temperature-controlled room to insure stable discharge rates. Two 0-1000 ohm and 0-5000 ohm helipots in series allowed the current to be varied from 0 to about 140 milli-amperes, depending on the resistance of the gold thermometer-heater. The heater current, I_H, was measured as the voltage drop across a 0.50002 ohm standard resistor calibrated by the National Bureau of Standards. A voltage divider, consisting of two wire-wound resistors of 115,000 ohms and 525 ohms in series was necessary because the entire voltage was too great to be measured by the potentiometer, which has a maximum range of 99,999 μv. The heater voltage, E_H, was measured across the 525 ohm resistor.

The voltage divider was calibrated in place by passing a small current from a mercury cell through it and measuring the potential drop across the battery and across the 525 ohm resistor of the voltage divider, thus obtaining $\frac{E_{total}}{E_{VD}} = 218.8369$. In order to measure R_{VD}, needed in the calculation of $\xi_{VD\ Loss}$, a standard volt-ohmmeter was used. The value of R_{VD} is so large (115500 ohms) that an error of as much as 500 ohm in R_{VD} results in a change of $\xi_{VD\ Loss}$ of less than 1 part in 10^6. Other uncertainties in the measurements are greater than this.

Thermometer voltage was supplied by two 2-volt Willard Type

DD5-1 cells connected in series. These cells are especially made to provide very stable discharges over long periods of time at low current drain. A 0-10,000 ohm resistor in series with a 10,000 ohm fixed resistor limited the current to 250 microamperes. The current, I_R, was measured as the voltage drop across a 100.001 ohm standard resistor calibrated by the National Bureau of Standards. The voltage drop across the resistance thermometer, E_R, was measured directly across the ends of the winding on the calorimeter can.

A 4 circuit master switch allowed simultaneous switching of the gold winding from the heater mode to the thermometer mode. (In Figure 4, these circuits are labelled W, X, Y, and Z.) Dummy resistors were placed in both the heater circuit and the thermometer circuit. These resistors were set at approximately the same value as the thermometer-heater, and allowed continuous discharge of the batteries. Interruptions would lead to unstable discharge and poor measurements.

Time was measured by an interval timer graduated in divisions of 0.001 minute, and connected to a 110 VAC, 60 hertz tuning fork. One circuit on the master switch was connected to the timer so that it was automatically started and stopped simultaneously with the power input.

III. OPERATING PROCEDURES

Due to the low value of Cp at lowest temperatures, the specimen used should be as large as possible. For this reason, the calorimeter was designed to accommodate about a 1000 gram sample. After loading the sample into the calorimeter can, the top is carefully soldered on with 60/40 solder leaving the pinhole open. Care must be used not to overheat the can and thereby damage the winding. A 000 soldering tip is very convenient for this purpose. Final touchup of the joint is done with a 500 watt soldering iron. A small amount of soldering paste aids in obtaining a good seal, but acid flux should never be used because of the possibility of corrosion. After sealing on the top, the can is placed in a vacuum desiccator, pumped out, and backfilled with 1 atm of 99.999% helium. The pinhole is rapidly sealed with a drop of solder after the desiccator lid is opened. A tinned surface expedites the closure. The entire can is weighed immediately after sealing and at intervals over a period of about 24 hours. Any leakage of helium would be detected as a weight gain. It is important that the can be tightly sealed, as air would condense at liquid hydrogen temperatures, giving erratic results, and temperature equilibration after heat input would be slow, leading to large errors. Rapid equilibration (usually within 5 minutes) is a further check on the validity of the seal.

After sealing, the calorimeter is suspended from the lower portion of the jacket with three linen cords. The cords pass through small

hangers machined on the top edge of the can. The Formvar insulated No. 40 leads are soldered to their terminals in as reproducible a manner as possible so as not to appreciably change their resistance. The calorimeter thermocouple is wound around the can, tied closely to the surface with silk thread, and its tip is inserted into the well provided for this purpose. The well was filled with Wood's metal (before installation of the thermocouple) to hold the tip securely and to maintain good thermal contact. A 500 watt soldering iron held on the bottom of the well for a few minutes heats the Wood's metal enough to melt it before insertion of the thermocouple. It is important to check that the calorimeter hangs plumb so that physical contact with the jacket is avoided. Verification of the electrical connections at each step is a good precaution and may avoid loss of time later.

The lower portion of the jacket is held in place by three 7/64 inch bolts extending through the upper portion. A tapered surface insures good physical contact between the upper and lower portions. The bolts are tightened in sequence to obtain good alignment. A thickness gauge and small machinist's level help in checking that the entire jacket assembly hangs plumb. A large threaded plug in the bottom may be removed to visually inspect the calorimeter after the jacket is in place to see that there is no physical contact between the jacket and calorimeter. The jacket heater lead, which is fiberglass insulated, is soldered to a terminal on the bottom of the jacket.

The outer Monel can is soldered into place using the minimum amount of heat to melt the solder. Water in the cup surrounding the stainless steel pipe prevents the temperature of the pipe from rising above 100°C and thus avoids damage to the insulation on the wires inside the pipe or to the linen cords suspending the jacket. As with the calorimeter can, only soldering paste is used for flux. It has been found helpful to support the can on a small screw jack during the soldering operation. Careful remelting of the solder with a very small flame after it has first cooled produces a smooth, tight joint.

If the calorimeter has not been exposed to air for more than 24 to 48 hours, pumpdown time to a pressure of 10^{-5} torr is about 1 to 2 days; otherwise adsorbed moisture lengthens this time by one or two additional days. After the pressure has reached 10^{-5} torr, heating the calorimeter two or three times to 310°K (about 10° above the highest temperature of measurement) helps in outgassing the system.

After the high-vacuum system has been sealed and pumped down, measurements are made in the temperature ranges 196°- 273°K and 273°- 300°K. For each specimen, measurements are made with first a dry ice-acetone slurry in the dewar, then ice-water, liquid nitrogen, and liquid hydrogen. With dry ice-acetone and ice-water, the dewar is not raised completely so that the ice can be replenished from the top. Small clamps on the support brackets prevent the dewar and can from falling down. By making measurements in this order, the low-

vacuum system need be sealed only once in each series.

On completion of measurements above 196°K, the dewar can be raised and the low-vacuum system sealed. It is extremely important that the bolts holding the outer can in place not be tightened excessively, otherwise damage to the joint may result. A light coating of high-vacuum silicone grease helps to obtain a reliable seal. The 16 bolts are tightened down in diametrically opposed pairs with a torque wrench, in increments of 25 in-lb, to a total tension of 150 in-lb. The seal is judged adequate if the vacuum as read on the exhaust gauge does not change perceptibly in two to four hours.

Liquid nitrogen is then introduced through the transfer line by pressurizing the supply dewar with 5-7 psi of helium. Back pressure on the system is vented to 2 psi by the exhaust valve. The dewar holds about 7 liters of liquid. Excessive frosting on the exhaust line and rapid boiloff signal the filling of the dewar with liquid nitrogen. When the dewar is full, about 1 torr of helium is admitted to the high-vacuum system (after closing the gate valve) to hasten the heat transfer and the cooling rate. An experience with a temporary increase in pressure in the high-vacuum system near 40°K shows the importance of insuring that condensible gases, such as oxygen or air, are removed from the lines by thorough flushing with helium before this operation. Under these conditions, the entire system cools from room temperature to 78°K in about 5 hours.

When the temperature has stabilized at 78°K, the dewar is topped off with liquid nitrogen, and the helium is pumped out of the high-vacuum system. With the high-speed diffusion pump, a pressure of 10^{-6} torr can be reached within 1/2 hour. Heat leak down the stainless steel pipe is small and is reduced by keeping the Monel cup full of dry ice and acetone. Liquid nitrogen consumption is very low—about 1 to 2 liters a day.

After measurements have been completed between 78°K and 196°K, the system is recooled to 78°K in preparation for the introduction of liquid hydrogen. Precooling with liquid nitrogen is necessary to prevent a large consumption and boil-off of liquid hydrogen. It has been found that normally one 25 liter dewar of liquid hydrogen is a very ample supply. When the temperature has reestablished at 78°K, the low-vacuum system is pressurized to about 5 psi with hydrogen. (The hydrogen is cooled by first passing it through a coil immersed in the dry ice-acetone slurry held in the Monel cup.) Helium cannot be used in this operation because it penetrates the pores in the glass dewar, rendering the dewar unsuitable for holding liquefied gases. The liquid nitrogen is discharged in about 30 minutes. Attempts to collect the liquid were unsuccessful because it boiled off too rapidly on passing through the uninsulated discharge tube. Immediately after discharging the liquid nitrogen, liquid hydrogen is transferred into the apparatus dewar. A pressure of 4 psi is sufficient for a rapid

transfer. Care was taken not to overfill the dewar, which would result in large and rapid evolution of hydrogen gas as well as in siphoning of the liquid back through the transfer line.

The apparatus cools from 78°K to 20.8°K in about 2 hours, after which the dewar is refilled. The Kinney pump is started, and the valve in the vacuum line is cautiously opened to allow the liquid to boil under reduced pressure. As the pressure drops over the liquid, the valve is gradually opened until the vacuum reaches 29 in. Hg. Two hours pumping is sufficient to reduce the temperature to about 18°K, after which the high-vacuum system is pumped out, and measurements up to about 80°K can be made. (Several more hours would be required to reach 14°K. The additional effort was judged to be unnecessary for purposes of this study, since the uncertainty in extrapolating the entropy is small at low temperatures.) Once 20°K is reached, the Kinney pump is turned off. Hydrogen consumption is about 1 inch on the liquid level indicator per hour. A full dewar is at 18 inches level, so that it is possible to make measurements over a period of 2 days, providing that one does not exhaust the hydrogen supply by pumping on it for too extended a period.

At the completion of the measurements, the liquid hydrogen is left to boil away before opening the low-vacuum system and disassembling the apparatus.

Safety Precautions for Liquid Hydrogen

The hazards in using liquid hydrogen stem from (1) the extreme explosion hazard in an atmosphere containing as little as 4% hydrogen by volume, and (2) the extreme coldness of the liquid. Therefore, considerable thought was given to designing the apparatus to incorporate as many safety features as possible. Thorough rehearsal and familiarity with every step in the operation, one of the best precautions, is highly recommended.

Since hydrogen rises rapidly to the highest point in the room, the calorimeter is located in a room which opens directly to the roof, thus eliminating collecting of hydrogen and buildup of an explosive concentration. In addition, an alarm sensor is mounted at the highest point in the room. The alarm has a loud horn, which is set to sound if at any time a concentration of hydrogen equal to 40% of the lower explosive limit is reached. All switching and measuring operations are done in a separate room so that personnel need be in the actual calorimeter room when hydrogen is present only during brief intervals, such as during transfer operations.

The buoyancy of hydrogen is taken into account in that the vacuum pumps and associated switches are located on the floor, below the level of the calorimeter assembly, and several feet away from the apparatus. The vacuum gauge box is at the far end of the room, about 10 feet from the calorimeter.

Two pressure relief valves insure against high pressures being built up in the system. All vent pipes, including those from vacuum pump exhaust ports, extend directly to the roof and outside the building.

Great care was taken to guard against sparking or static charge buildup during the period when hydrogen is in the room. The apparatus is well grounded electrically. The supply dewar is also grounded by a strap clipped onto its neck. No tools are allowed in the vicinity of the calorimeter with hydrogen present. Personnel wear grounding straps on their shoes and avoid wearing synthetic or wool clothing on days when working with liquid hydrogen. No switching operations take place with hydrogen present—vacuum pumps, gauges, etc., are turned on before the supply dewar is brought into the room.

Only a few drops of liquid hydrogen will give rise to a large quantity of vapor; therefore, measures must be taken to avoid spilling or splashing the liquid. Experience has been that perhaps 1 or 2 cc of liquid releases enough vapor to sound the alarm. The supply dewar is thus moved slowly and carefully. It is gently lifted over door sills, bumps, etc. The transfer line is lowered slowly into the liquid to allow it to cool and to prevent splashing of the liquid. Care is taken to prevent overfilling of the dewar, which would lead to siphoning of the liquid back through the transfer line. The liquid level indicator is very helpful in this. The transfer line is withdrawn slowly to allow it to drain before completely removing it from the supply

dewar. When not in use, the transfer line is closed off by a clamped rubber hose over the end.

A secondary hazard in the use of liquid hydrogen is its very low temperature. At -253°C, anything coming into contact with it is immediately and thoroughly frozen. Protective gloves and safety glasses are worn when handling any of the apparatus coming into contact with the liquid, or when moving the dewar.

Before being used with hydrogen, the apparatus was checked and approved by the Lawrence Radiation Laboratory Hydrogen Safety Committee. Experience with liquid hydrogen and respect for its hazardous properties have made its use thus far free from mishap.

IV. MEASUREMENT AND CALCULATION METHODS

Measurement

The previous section has described in some detail the construction and preparation of the apparatus for making the measurements. This section describes how the measurements are made and how the results are calculated. Much of what is described here is based on the experiences of Giauque and his coworkers, as summarized by Giauque in a set of unpublished notes.[20] Significant changes in Giauque's experimental procedure have been made, however, especially after some experience in the operation of the calorimeter. Changes have also been made in the calculation method.

The basic method of heat capacity measurements is to inject a measured amount of energy into the sample and to measure the resulting temperature rise. At low temperatures, where the Cp is changing rapidly, the energy input, ξ , is adjusted so that the temperature rise of the calorimeter, ΔT_c, is of the order of 1°. As the slope of the Cp curve decreases, ΔT_c is gradually increased to about 4°. The spacing between runs also increases from 2° at lowest temperatures to 7° or 8° near room temperature. ξ can be increased by varying both the heating rate and the length of the heating interval.

Figure 5 is a time-temperature plot of a typical run. Reference to it will greatly facilitate understanding the following discussion. The jacket, being of considerable mass, provides an effective iso-

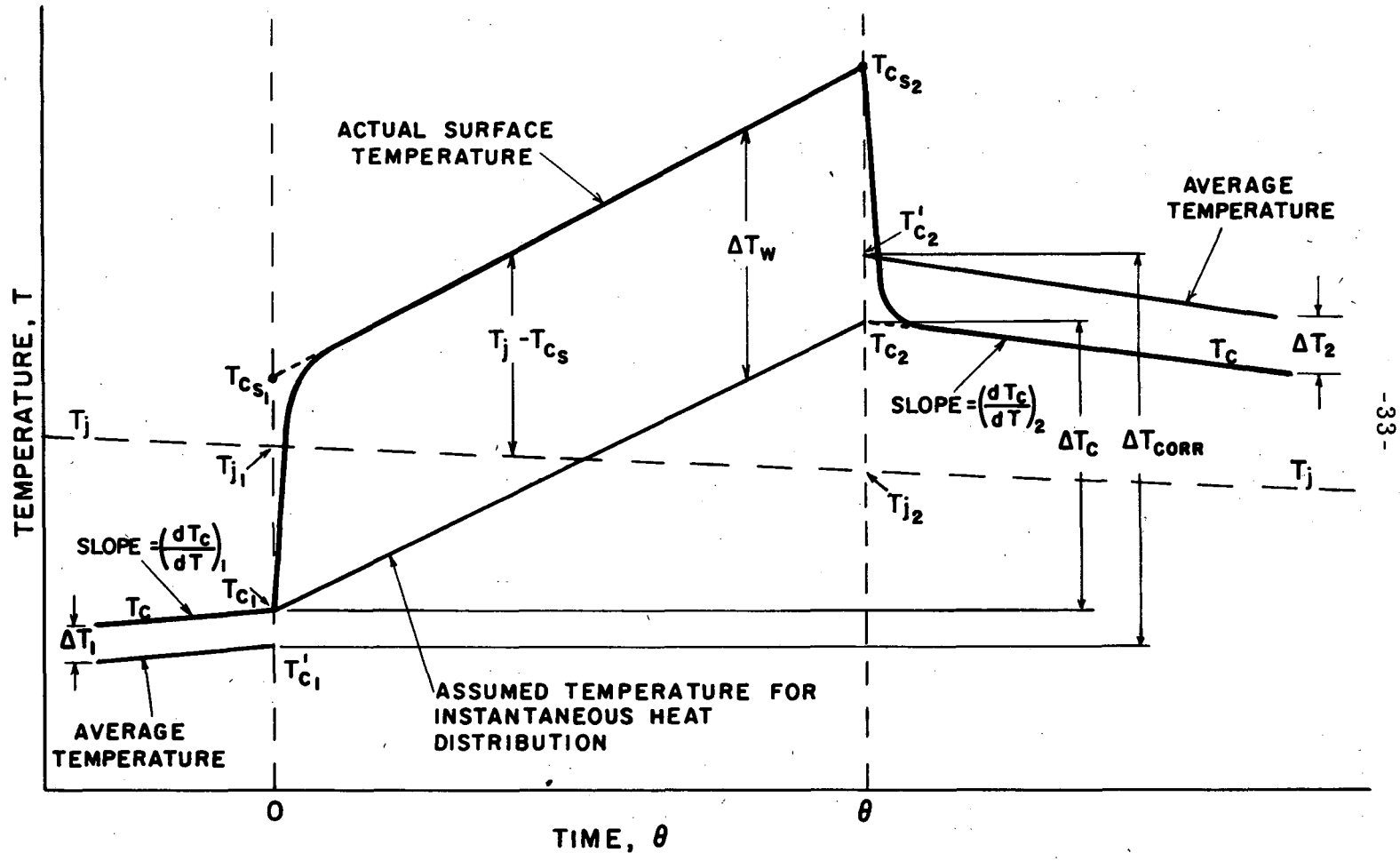

FIGURE 5. TIME-TEMPERATURE DISTRIBUTION FOR A TYPICAL RUN.

XBL 6912-6635

thermal surrounding for the calorimeter. At the start of a run, its temperature, T_j, is adjusted to be approximately midway between the initial temperature of the calorimeter, T_{c_1}, and the anticipated final temperature, T_{c_2}. Since the jacket is hotter than the calorimeter, the calorimeter temperature will slowly drift upward. Alternating measurements at 1/2 minute intervals of the resistance thermometer voltage, E_R, and thermometer current, I_R, over a period of several minutes establishes the drift rate of the resistance of the gold winding and, hence, the calorimeter temperature. Galvanometer readings are plotted as soon as they are read to be certain that the drift is linear, allowing precise graphical extrapolation to T_{c_1}.

When the resistance drift rate has been well established, calorimeter heating is started. During the heating time, measurements are made of heater current, I_H, and heater voltage, E_H. These values are not constant because both the battery voltage and heater resistance are changing as the temperature rises. I_H and E_H are measured alternately at 1/2 or 1 minute intervals. T_c is also checked as the run nears completion, and the time of power input is shortened or lengthened as needed to make the actual temperature rise approximate the desired value.

After the power is turned off, measurements of E_R and I_R are made in the same way as before the heating period until the final drift rate is established, allowing extrapolation to T_{c_2}. Since the calorim-

eter is now hotter than the jacket, the final temperature drift rate will be negative.

The jacket temperature is only approximately constant during a run. It usually drifts a few hundredths of a degree, and so measurements of initial and final jacket temperatures, T_{j_1} and T_{j_2}, are made with the jacket thermocouple to allow correction for jacket drift to be made. The jacket drift rate increases as the jacket temperature gets further away from the temperature of the substance in the dewar. As the temperature rises, the vacuum slowly gets poorer, increasing the rate of heat conduction and hence, the rate of change of T_j.

Thermometry

A gold resistance thermometer is used to measure the temperature of the calorimeter rather than a thermocouple because its temperature coefficient is far greater than that of a thermocouple. Greater precision in temperature measurement is thus possible. The resistance thermometer also has the advantage of being wound over nearly the entire length of the calorimeter can, whereas a thermocouple is inserted at only one point; thus, small local fluctuations in temperature, caused, perhaps, by poor thermal contact of the specimen, tend to be averaged out. The disadvantages of the resistance thermometer are that it is not a strain-free device and that its resistance changes slightly from one series of runs to another due to a slight unreproducibility of the solder connections, thus requiring

frequent checks on its calibration. Fortunately, this can be accomplished without excessive additional effort by means of the calibrated copper-constantan calorimeter thermocouple.

The gold thermometer was originally calibrated, and its calibration was routinely checked, by first making the jacket temperature as nearly as possible equal to the calorimeter temperature. In this way, an equilibrium condition is reached after a short wait. Measurements are then made of E_R, I_R, and T_c (using the thermocouple) over a period of a few minutes to insure that the temperature of the calorimeter is not drifting. Comparison of values of R calculated from these data with the temperature as measured by the thermocouple yields a set of values of R versus T. The same thermocouple used by Huffstutler[15] was used in the present investigation, eliminating the need for calibrating the thermocouple. Huffstutler calibrated the copper-constantan thermocouple against a platinum resistance thermometer calibrated by the National Bureau of Standards.

The R-T values were fitted by a CDC6400 computer to a series of Debye functions, as described by Giauque,[20] to produce a table of values of R and $\frac{dR}{dT}$ as a function of T at 0.1°K intervals from 10° to 310°K. Temperatures to the nearest 0.01°K were obtained from this table by interpolation.

Calculations

The average values of E_H and I_H, $\widetilde{E}_H$ and $\widetilde{I}_H$, respectively, are

obtained by plotting readings of E_H and I_H versus heating time, and averaging the values obtained at 0.21θ and 0.79θ, where θ is the heating time. This method allows for either linear or quadratic drift of the voltage and current, and is derived by Gibson and Giauque.[17] A plot for a typical run is shown in Figure 6. The total energy input is:

$$\xi = \tilde{E}_H \cdot \tilde{I}_H \cdot \theta. \qquad (1)$$

But only a fraction of the total voltage is measured due to the voltage divider (see page 21) and therefore:

$$\tilde{E}_H(\text{true}) = 218.8369\,\tilde{E}_H(\text{measured}). \qquad (2)$$

I_H is measured as the voltage drop across a standard 0.5 ohm resistor, so by Ohm's Law:

$$\tilde{I}_H = \frac{\tilde{I}(\text{measured})}{0.50002} \qquad (3)$$

substituting (2) and (3) into (1) and making the appropriate unit conversions gives the total energy input:

$$\xi = 2.62594 \times 10^{-2}\tilde{E}_H \cdot \tilde{I}(\text{measured}) \cdot \theta \qquad (4)$$

where $\tilde{E}_H$ and $\tilde{I}$ are in millivolts, θ is in minutes, and ξ is in joules.

Small, but significant, amounts of power are dissipated in the voltage divider and in the No. 40 leads to the calorimeter, and must be corrected for. (The power loss in the No. 30 leads was judged to be insignificant.) The voltage divider loss is:

$$\xi_{\text{VD loss}} = E_{VD} \cdot I_{VD} \cdot \theta = \frac{E_{VD}^2 \cdot \theta}{R_{VD}}. \qquad (5)$$

Substitution of the value of R_{VD} and (2), into (5), and converting for

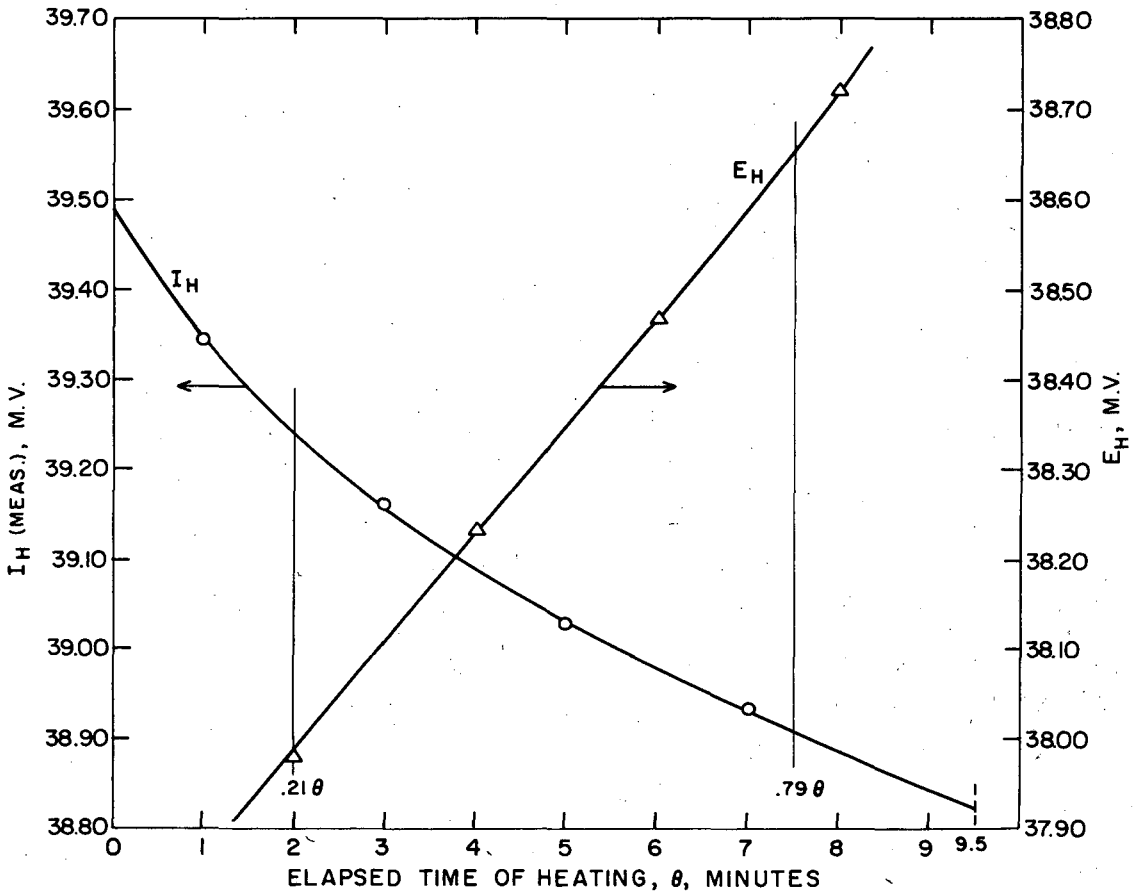

FIGURE 6 HEATER CURRENT AND VOLTAGE FOR A TYPICAL RUN.

XBL 6912-6636

units gives:

$$\xi_{VDloss} = 2.48777 \times 10^{-5}(\tilde{E}_H)^2 \cdot \theta \qquad (6)$$

where ξ is in joules, $\tilde{E}_H$ in millivolts, and θ in minutes.

Joule heating of the No. 40 leads occurs throughout the heating interval. However, the calorimeter is warmer than the jacket during half of the run and cooler during the other half. Therefore heat is flowing to the calorimeter due to the joule heating only during half of the run; during the other half of the run it is flowing toward the jacket. This is most easily accounted for by assuming the No. 40 leads are only 8.6 cm long, instead of their true length of 17.2 cm. The power loss from this cause is:

$$\xi_{\#40} = E_{40} \cdot I_{40} \cdot \theta = (\tilde{I}_H)^2 R_{40} \theta \,. \qquad (7)$$

Substituting (2) and (3) into (7) and converting to consistent units gives:

$$\xi_{\#40} = 2.39981 \times 10^{-4}(\tilde{I}_H)^2 R_{40} \theta \,. \qquad (8)$$

R_{40}, the resistance of 8.6 cm of No. 40 wire was calculated as a function of temperature from data given in the literature.[21] Above 85°K it was found that the following linear relationship applied:

$$R_{40}(\text{ohms}) = 0.001169T(°K) - 0.0562 \,. \qquad (9)$$

Below 85°K, the resistance was obtained directly from a graph. The corrected energy input is then obtained by subtracting the sum of (6) and (8) from (4).

The temperature rise, ΔT_c, is obtained from the values of E_R and I_R extrapolated to the beginning and ending times of the heating

interval. Figure 7 shows this extrapolation for a typical run. The thermometer current is measured as the voltage drop across a standard 100 ohm resistor, so that:

$$I_R(\text{true}) = \frac{I_R(\text{measured})}{100.001} \quad . \tag{10}$$

Substitution of (10) into Ohm's Law gives the resistance:

$$R = \frac{E}{I} = \frac{100.001\, E_R}{I_R(\text{measured})} \quad . \tag{11}$$

The temperature corresponding to the measured resistance is obtained by linear interpolation in the table of R vs T. Since the temperature changes during a measurement, the temperature of measurement is taken as the average of the beginning and final temperatures.

Division of corrected energy input by ΔT_c, obtained by subtracting the initial temperature from the final, gives a first approximation to Cp. Corrections to both the enrgy and temperature rise are small (less than 5%) and arise from 3 sources:

(1) Permanent heat leak along the wires and supports,

(2) Newton's Law heat transfer due to differences in temperature between the jacket and calorimeter, and

(3) The surface temperature during a run is higher than the average temperature due to the fact that the heating wire is wound around the outside of the can, and heat is not distributed instantaneously during heating.

We first consider the various sources of energy supplied to the

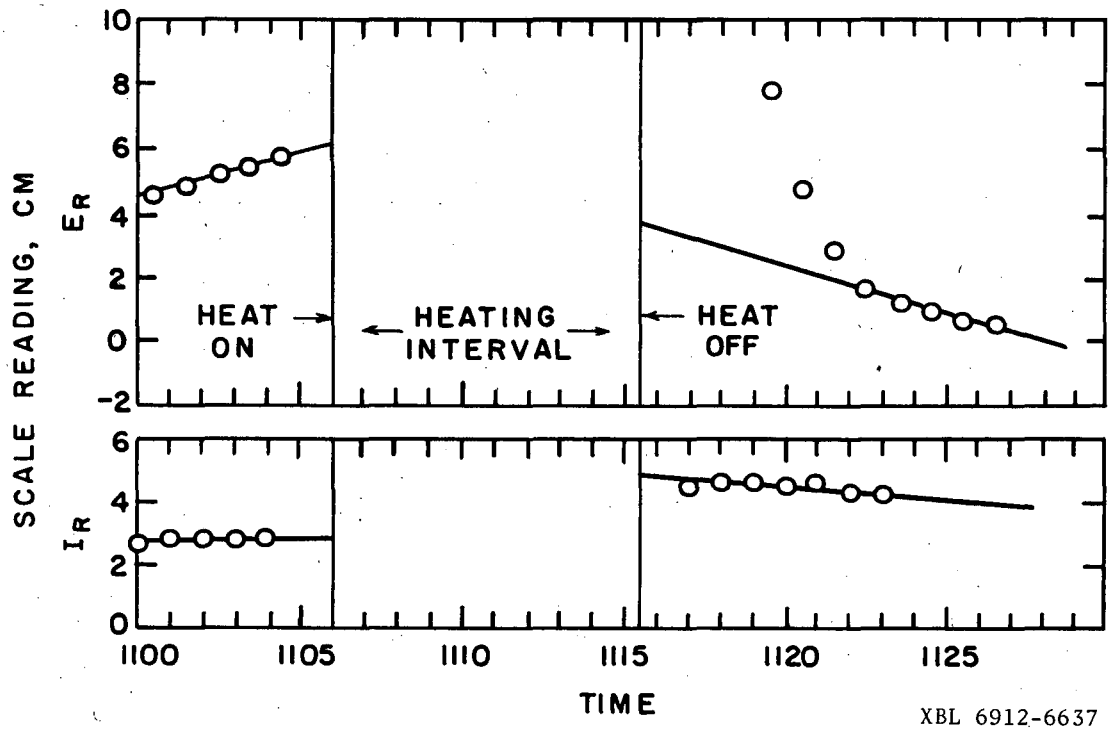

FIGURE 7 THERMOMETER VOLTAGE AND CURRENT READINGS FOR A TYPICAL RUN.

calorimeter during the run. Heat can be supplied

(1) electrically, denoted $\frac{dE}{dt}$,

(2) by Newton's Law heat transfer, denoted $\frac{dH_N}{dt}$, and

(3) by heat leaking along the wires and supports, denoted $\frac{dH_L}{dt}$.

The average total heat during the run is the sum of these 3 quantities:

$$\left(\frac{dH}{dt}\right)_{avg} = \left(\frac{dE}{dt}\right)_{avg} + \left(\frac{dH_N}{dt}\right)_{avg} + \left(\frac{dH_L}{dt}\right)_{avg} . \qquad (12)$$

but $\frac{dH}{dt} = Cp\frac{dT_c}{dt}$, so that:

$$Cp_{avg}\left(\frac{dT_c}{dt}\right)_{avg} = \left(\frac{dE}{dt}\right)_{avg} + \left(\frac{dH_N}{dt}\right)_{avg} + \left(\frac{dH_L}{dt}\right)_{avg} . \qquad (13)$$

In general, Newton's Law can be written:

$$\frac{dH_N}{dt} = B_N\left(T_j - T_c\right), \qquad (14)$$

where B_N is the Newton's Law constant, T_j is the temperature of the jacket, and T_c is the temperature of the calorimeter. Assuming that the permanent heat leak is constant, equations (13) and (14) can be combined into two equations, applying for periods before and after heating, where $\frac{dE}{dt} = 0$:

$$Cp_1\left(\frac{dT_c}{dt}\right)_1 = B_N\left(T_{j_1} - T_{c_1}\right) \qquad (15)$$

$$Cp_2\left(\frac{dT_c}{dt}\right)_1 = B_N\left(T_{j_2} - T_{c_2}\right) . \qquad (16)$$

Subtracting (16) from (15) and solving for B_N gives:

$$B_N = \frac{Cp_1\left(\frac{dT_c}{dt}\right)_1 - Cp_2\left(\frac{dT_c}{dt}\right)_2}{\left(T_{j_1} - T_{c_1}\right) - \left(T_{j_2} - T_{c_2}\right)} \quad . \tag{17}$$

As a first approximation, let $Cp_1 = Cp_2 = Cp_{approx} = \frac{\xi}{T_{c_2} - T_{c_1}}$

Then:

$$B_{N_{approx}} = \frac{\xi\left[\left(\frac{dT_c}{dt}\right)_1 - \left(\frac{dT_c}{dt}\right)_2\right]}{\left(T_{c_2} - T_{c_1}\right)\left[\left|T_{j_1} - T_{j_2}\right| + \left|T_{c_2} - T_{c_1}\right|\right]} \quad . \tag{18}$$

Having obtained an approximate value for the Newton's Law constant B_N, we must now evaluate the heat leak into or out of the calorimeter. This arises from two sources: permanent heat leak along the wires and supports, and Newtonian heat transfer (see Equation 12). We combine the total heat leak from these two sources into one quantity, ΔH_{N+L}. Returning to Equations (13) and (14), we can write two equations for the periods before and after heating:

$$Cp_1\left(\frac{dT_c}{dt}\right)_1 = \left(\frac{dH_L}{dt}\right)_1 + B_N\left(T_{j_1} - T_{c_1}\right) \tag{19}$$

$$Cp_2\left(\frac{dT_c}{dt}\right)_2 = \left(\frac{dH_L}{dt}\right)_2 + B_N\left(T_{j_2} - T_{c_2}\right). \tag{20}$$

We now assume that instead of being constant, the heat leak varies linearly with time, so that:

$$\left(\frac{dH_L}{dt}\right)_{avg} = \frac{1}{2}\left[\left(\frac{dH_L}{dt}\right)_1 + \left(\frac{dH_L}{dt}\right)_2\right] \quad . \tag{21}$$

Adding (19) and (20), substituting (21) into the resulting equation, and rearranging, gives:

$$\left(\frac{dH_L}{dt}\right)_{avg} = \frac{1}{2}\left[Cp_1\left(\frac{dT_c}{dt}\right)_1 + Cp_2\left(\frac{dT_c}{dt}\right)_2\right] - \frac{1}{2}B_N\left[\left(T_{j_1}-T_{c_1}\right)+\left(T_{j_2}-T_{c_2}\right)\right]. \quad (22)$$

Note that this equation is valid for all periods of the run—both before and after heating as well as during heating.

Newton's Law of heat transfer states that the rate of heat transfer between two surfaces is directly proportional to the temperature difference of the surfaces. Therefore, Newton's Law during electrical heating becomes:

$$\left(\frac{dH_N}{dt}\right)_{avg} = B_N\left(T_j - T_{c_s}\right)_{avg}, \quad (23)$$

where T_{c_s} is the surface temperature of the calorimeter. Assuming that the surface temperature varies linearly, which is borne out in practice, we can write:

$$\left(\frac{dH_N}{dt}\right)_{avg} = \frac{1}{2}B_N\left[\left(T_{j_1}-T_{c_{s_1}}\right)+\left(T_{j_2}-T_{c_{s_2}}\right)\right]. \quad (24)$$

Referring to Figure 5, the surface temperatures of the calorimeter at the beginning and end of the run are:

$$T_{c_{s_1}} = T_{c_1} + \Delta T_w \quad (25)$$

$$T_{c_{s_2}} = T_{c_2} + \Delta T_w, \quad (26)$$

where ΔT_w is the difference between the surface temperature and the assumed instantaneous temperature. Substituting (25) and (26) into (24) gives:

$$\left(\frac{dH_N}{dt}\right)_{avg} = \frac{1}{2} B_N \left[\left(T_{j_1} - T_{c_1}\right) + \left(T_{j_2} - T_{c_2}\right)\right] - B_N \Delta T_w \quad (27)$$

Adding (22) and (27) :

$$\left(\frac{dH_L}{dt}\right)_{avg} + \left(\frac{dH_N}{dt}\right)_{avg} = \frac{1}{2}\left[Cp_1\left(\frac{dT_c}{dt}\right)_1 + Cp_2\left(\frac{dT_c}{dt}\right)_2\right] - B_N \Delta T_w \quad (28)$$

or ,

$$\Delta H_{N+L} = \frac{1}{2}\theta\left[Cp_1\left(\frac{dT_c}{dt}\right)_1 + Cp_2\left(\frac{dT_c}{dt}\right)_2\right] - B_N \Delta T_w \theta \quad . \quad (29)$$

Again approximating $Cp_1 = Cp_2 = Cp_{approx} = \frac{\xi}{T_{c_2} - T_{c_1}}$ and substituting (18):

$$\Delta H_{N+L} = \frac{1}{2}\frac{\xi\,\theta}{T_{c_2} - T_{c_1}}\left[\left(\frac{dT_c}{dt}\right)_1 + \left(\frac{dT_c}{dt}\right)_2\right] - \left(\frac{\xi\theta\Delta T_w}{T_{c_2} - T_{c_1}}\right)\left[\frac{\left(\frac{dT_c}{dt}\right)_1 - \left(\frac{dT_c}{dt}\right)_2}{\left(T_{j_1} - T_{j_2}\right) + \left(T_{c_2} - T_{c_1}\right)}\right]$$

$$= \frac{\xi\,\theta}{T_{c_2} - T_{c_1}}\left\{\frac{\left(\frac{dT_c}{dt}\right)_1 + \left(\frac{dT_c}{dt}\right)_2}{2} - \frac{\Delta T_w\left[\left(\frac{dT_c}{dt}\right)_1 - \left(\frac{dT_c}{dt}\right)_2\right]}{\left(T_{j_1} - T_{j_2}\right) + \left(T_{c_2} - T_{c_1}\right)}\right\} \quad . \quad (30)$$

ΔH_{N+L} is the total correction to the energy. A correction must also be applied to the temperature difference due to the fact that the surface temperatures as measured by the resistance thermometer differ slightly from the average temperature of the calorimeter. See Figure 5. Before heating, the surface is warmer than the average temperature T_{c_1} ' because heat is being supplied to it by heat transfer to the jacket. Similarly, after heating the surface is cooler than the average temperature T_{c_2} '. Since the surface temperature is propor-

tional to the heating rate, as assumed by Giauque,[20]

ΔT_w is due to $\frac{\xi}{\theta}$ joules per minute heating

ΔT_1 is due to $\left(\frac{dH_N}{dt}\right)_1$ joules per minute heating

ΔT_2 is due to $\left(\frac{dH_N}{dt}\right)_2$ joules per minute cooling

where $\Delta T_1 = \left|T_{c_1} - T_{c_1}'\right|$ and $\Delta T_2 = \left|T_{c_2} - T_{c_2}'\right|$. (The absolute value sign is inserted because $\left(\frac{dH_N}{dt}\right)_2$ is a negative quantity when the surface is cooling.) Since the temperature differences are proportional to heating rate:

$$\frac{\Delta T_w}{\left(\frac{\xi}{\theta}\right)} = \frac{\Delta T_1}{\left(\frac{dH_N}{dt}\right)_1} = \frac{\Delta T_2}{\left|\left(\frac{dH_N}{dt}\right)_2\right|} \quad . \tag{31}$$

Cross multiplying:

$$\Delta T_1 = \frac{\Delta T_w \left(\frac{dH_N}{dt}\right)_1 \theta}{\xi} \tag{32}$$

$$\Delta T_2 = \frac{\Delta T_w \left|\left(\frac{dH_N}{dt}\right)_2\right| \theta}{\xi} \quad . \tag{33}$$

Therefore,

$$T_{c_2}' = T_{c_2} + \Delta T_2 = T_{c_2} + \frac{\Delta T_w \theta}{\xi}\left(\frac{dH_N}{dt}\right)_2 \tag{34}$$

$$T_{c_1}' = T_{c_1} - \Delta T_{c_1} = T_{c_1} - \frac{\Delta T_w \theta}{\xi}\left|\left(\frac{dH_N}{dt}\right)_1\right| \tag{35}$$

Subtracting (35) from (34):

$$T_{c_2}' - T_{c_1}' = \left(T_{c_2} - T_{c_1}\right) + \frac{\Delta T_w \theta}{\xi}\left[\left(\frac{dH_N}{dt}\right)_1 + \left|\left(\frac{dH_N}{dt}\right)_2\right|\right] \tag{36}$$

But

$$\frac{1}{2}\left[\left(\frac{dH_N}{dt}\right)_1 + \left(\frac{dH_N}{dt}\right)_2\right] = \left(\frac{dH_N}{dt}\right)_{avg} \quad (37)$$

Substituting $Cp_{avg} = \dfrac{\left(\frac{dH}{dt}\right)_{avg}}{\left(\frac{dT}{dt}\right)_{avg}}$ into (37) gives:

$$\frac{1}{2}\left[\left(\frac{dH_N}{dt}\right)_1 + \left(\frac{dH_N}{dt}\right)_2\right] = Cp_{avg}\left(\frac{dT}{dt}\right)_{avg} = \tfrac{1}{2}Cp_{avg}\left[\left(\frac{dT_c}{dt}\right)_1 + \left(\frac{dT_c}{dt}\right)_2\right]. \quad (38)$$

Substituting (38) into (36):

$$T_{c_2}' - T_{c_1}' = \Delta T_{corr} = \left(T_{c_2} - T_{c_1}\right) + \frac{\Delta T_w \theta Cp_{avg}}{\xi}\left[\left(\frac{dT_c}{dt}\right)_1 + \left(\frac{dT_c}{dt}\right)_2\right] \quad (39)$$

But $\xi = Cp_{avg}\left(T_{c_2} - T_{c_1}\right)$ so that:

$$\Delta T_{corr} = \left(T_{c_2} - T_{c_1}\right) + \frac{\Delta T_w \cdot \theta}{T_{c_2} - T_{c_1}}\left[\left(\frac{dT_c}{dt}\right)_1 + \left(\frac{dT_c}{dt}\right)_2\right]. \quad (40)$$

The second approximation to Cp then becomes:

$$Cp = \frac{\xi + \Delta H_{N+L}}{\Delta T_{corr}}, \quad (41)$$

where ΔH_{N+L} is calculated from (30), and ΔT_{corr} from (40). If desired, a further approximation to Cp can be made by plotting the Cp values obtained from (41) against absolute temperature and reading off Cp_1 and Cp_2 at the beginning and ending temperatures for each run. These values are then substituted into the following equations to obtain a more exact value for Cp:

$$B_N = \frac{Cp_1\left(\frac{dT_c}{dt}\right)_1 - Cp_2\left(\frac{dT_c}{dt}\right)_2}{\left(T_{j_1} - T_{j_2}\right) + \left(T_{c_2} - T_{c_1}\right)} \qquad (42)$$

$$\Delta H_{N+L} = \frac{1}{2}\theta\left[Cp_1\left(\frac{dT_c}{dt}\right)_1 + Cp_2\left(\frac{dT_c}{dt}\right)_2\right] - B_N \Delta T_w \theta \qquad (43)$$

$$\Delta T_{corr} = \left(T_{c_2} - T_{c_1}\right) + \frac{\Delta T_w \theta}{\xi}\left[Cp_1\left(\frac{dT_c}{dt}\right)_1 + Cp_2\left(\frac{dT_c}{dt}\right)_2\right] \qquad (44)$$

In practice, it was found that the second approximation gave sufficiently accurate values of Cp because the temperature interval of a run was sufficiently small so that the curvature in Cp over the interval was negligible. For the same reason, the "curvature correction", described by Westrum,[22] was not needed.

After measuring the total Cp, the Cp of the calorimeter was subtracted, and small corrections were made for the amounts of helium in the calorimeter and the solder used in sealing the top. The helium was assumed to be an ideal gas with $C_v = \frac{3}{2}R$ at all temperatures. This correction was small—about 0.06 cal/deg with a sample and 0.16 cal/deg with the empty calorimeter.

The solder correction arises from the fact that it is impossible to solder the top with precisely the same amount of material each time the sample is changed. The amount of solder used to seal the empty calorimeter was taken as the base weight. Knowing the weight of the empty calorimeter, the sample, and the helium, the deviation of the weight of solder from the base weight could be calculated for each

series of runs. The Cp of solder was calculated from the literature values for pure lead and pure tin,[2] assuming Kopp's Law and the composition of the solder to be 60% Sn by weight.

V. MATERIALS

Pure Metals

99.999+% gold was obtained from Cominco American, Inc., and 99.999+% copper was obtained from American Smelting and Refining Company. For both metals, all impurities were below the 1 ppm level except that the copper had 2 ppm tellurium impurity.

Alloy Preparation

After measurements had been completed on pure gold, the AuCu alloy was prepared. Enough pure gold and pure copper were weighed out to make approximately 7 g-atoms of alloy. The mixture was melted in an induction furnace under helium at 1200°C in a graphite crucible, then poured into a chilled copper mold to form an ingot 1 inch in diameter and 6 inches long. A few drops of the liquid mixture were spilled when pouring, so that the final weight was 15 grams less than the combined weights of the pure metals. The lattice parameter of the alloy agreed well with that predicted from the pure metals, so the composition was taken to be 50 atomic % Au, and 50 atomic % Cu.

The resulting ingot was cold worked slightly by rolling, sealed into an evacuated quartz tube and homogenized at 590°C for 12 days, then quenched into an ice-brine bath. It had been planned to roll and swage the ingot to about 1/8 inch to 1/4 inch diameter rods for heat treatment; however, the ingot showed signs of extensive cracking after three passes through the rolling mill, so this attempt was abandoned,

and the ingot was sawed into rods 1/4 inch square X 5 inches long.

The rods were resealed under vacuum in a quartz tube, held at 365°C for 5 days, then slowly cooled to about 200°C over a period of 4 days by reducing the temperature about 25° every 12 hours. Since filings for a powder pattern would not have the same degree of order as the original sample, the rods were X-rayed without taking filings. The X-ray diffraction pattern showed sharp superlattice lines with a well defined simple tetragonal structure, indicating that the sample was well ordered.

After measuring the Cp of the ordered state, the rods were sealed again into quartz. To insure rapidity of quenching, each rod was individually sealed into a tube. Five small pellets suitable for heat of formation measurements were placed into five of the sample tubes. Since they were given the same heat treatment and quench as the rods, the degree of order of the rods and the pellets should be the same, and characterization of the samples by heat of formation measurements is a valid porcedure. All tubes were then heated to 475± 2°C for 9 days and quenched one by one into an ice-brine bath. All the tubes except one shattered on contact with the ice bath, indicating the quenching was extremely rapid. The X-ray pattern of the quenched rods showed no evidence of any superlattice lines, indicating the absence of long-range order. The rod in the tube which remained intact had a significantly more exothermic heat of formation (see next section), and consequently

was not used in any measurements.

VI. RESULTS

Pure Gold

Seventy-two runs were made on pure gold. The sample weighed 1252.456 g = 6.3587 g-atoms. The experimental results are given in Table I and smoothed values in Table II. The results are also shown on Figure 8.

Previous measurements on gold avove 15°K have been made by Franzosini,[23] Geballe and Giauque,[24] and Clusius and Harteck.[25] The present values agree well with the previous data except in the temperature range between 70° and 150°K where the present data are 0.5 - 1.0% high. (On Figure 8, the values chosen by Hultgren, et al.[2] are indicated as a solid line.) Integration of the values obtained in this study yields $S^\circ_{298.15}$ = 11.397 e.u., of which 0.012 e.u. are extrapolated below 20°K, and $H^\circ_{298.15} - H^\circ_0$ = 1440 cal/deg. Hultgren's[2] values for the entropy and heat difference are, respectively, 11.352(±0.05) e.u. and 1438 cal/deg. No explanation for the small deviation is apparent.

Very little scatter in the data is evident below about 200°K. Above that temperature, there is a slight increase in the amount of scatter. The precision of the data is within 0.2% to 200°K, and within 0.5% thereafter. The same general trend was observed in all the measurements. Impurities in the helium used to back-fill the calorimeter may be responsible for this effect. In particular, moisture would freeze

TABLE I. Experimental Values for Pure Gold

T, °K	Cp, cal/g-atom-deg	T, °K	Cp, cal/g-atom-deg
19.68	0.656	198.57	5.818
21.61	0.876	202.64	5.833
24.22	1.182	202.69	5.836
27.36	1.602	206.74	5.811
27.50	1.624	210.51	5.914
30.88	2.013	210.84	5.867
31.34	2.035	214.31	5.879
35.48	2.365	214.90	5.884
42.69	2.934	215.95	5.860
49.70	3.446	219.81	5.848
58.75	3.985	222.21	5.841
68.54	4.414	223.91	5.876
73.89	4.616	227.61	5.928
78.45	4.675	231.44	5.886
80.79	4.824	232.03	5.886
82.86	4.878	235.06	5.882
85.32	4.931	235.65	5.912
91.14	5.057	238.81	5.915
96.06	5.125	239.49	5.946
101.38	5.195	242.55	5.889
106.55	5.273	243.19	5.900
111.61	5.323	246.83	5.896
116.56	5.428	247.06	5.993
121.40	5.439	251.24	5.909
127.02	5.474	255.35	5.969
131.67	5.534	258.16	6.016
136.23	5.563	264.44	5.921
143.29	5.627	267.96	5.959
153.05	5.667	273.89	5.973
158.48	5.709	277.38	5.983
163.78	5.732	277.76	5.977
168.95	5.729	281.54	6.015
176.95	5.785	284.00	5.980
181.89	5.753	285.74	6.013
187.49	5.795	290.88	5.998
191.47	5.785	295.70	6.034

TABLE II. Smoothed Values for Pure Gold

T, °K	Cp, cal/g-atom-deg	T, °K	Cp, cal/g-atom-deg
20	0.700	130	5.513
25	1.230	140	5.588
30	1.781	150	5.649
35	2.273	160	5.701
40	2.712	170	5.746
45	3.119	180	5.782
50	3.474	190	5.813
55	3.783	200	5.839
60	4.056	210	5.861
65	4.287	220	5.882
70	4.481	230	5.900
75	4.646	240	5.919
80	4.784	250	5.937
85	4.902	260	5.955
90	5.008	270	5.973
95	5.100	280	5.993
100	5.181	290	6.012
110	5.317	298.15	6.027
120	5.425	300	6.029

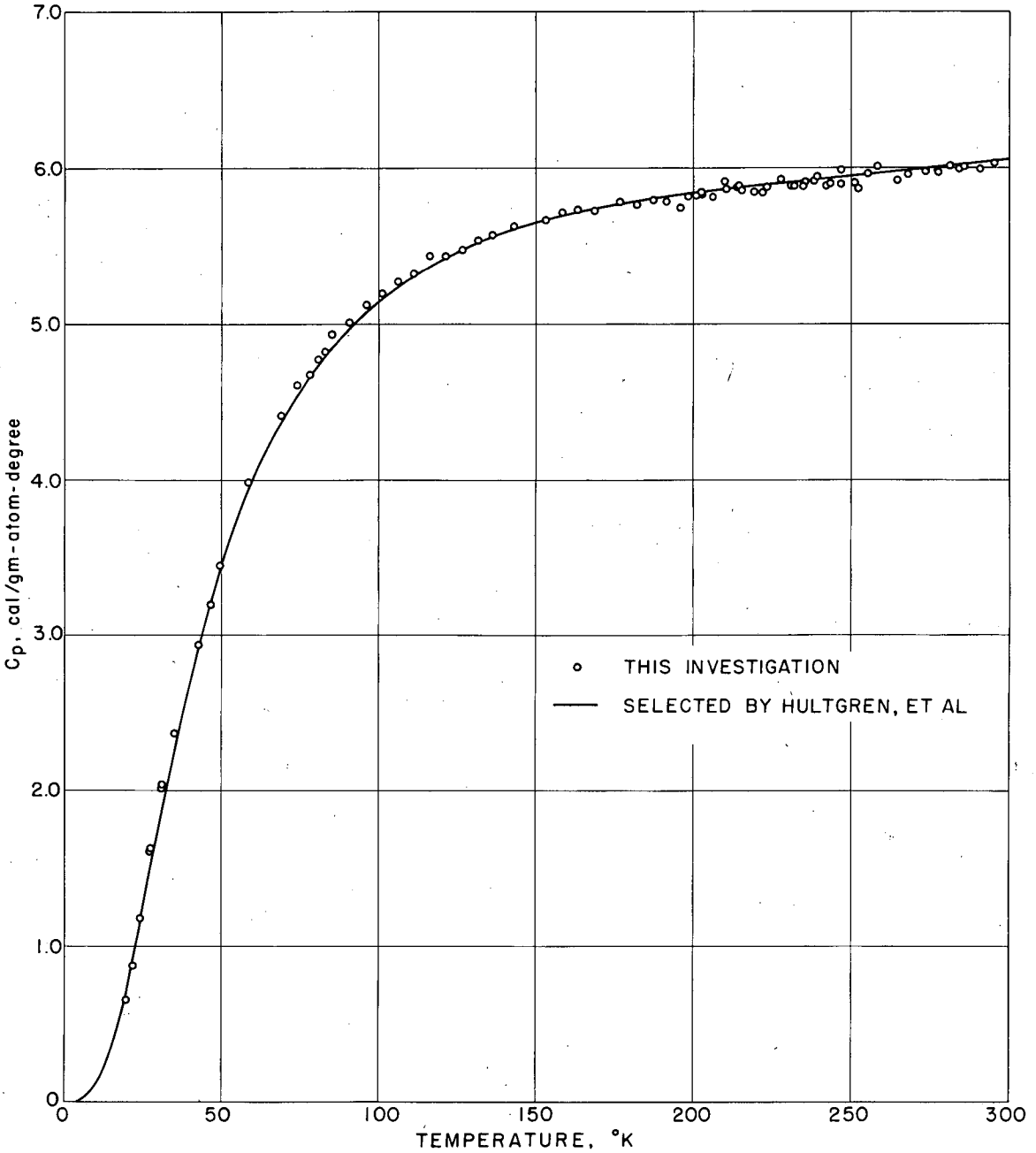

FIGURE 8 HEAT CAPACITY OF GOLD.

XBL 6912-6642

below 273°K, and would, if present, greatly increase the scatter above that temperature, because some of the energy supplied to the calorimeter would be used in melting the ice rather than in heating the sample. By the same token, CO_2 would have an effect above 196°K.

Calorimeter

Fifty-eight runs were made on the "empty" calorimeter (which had been filled with helium at approximately 1 atmosphere). Experimental data are presented in Table III.

Alloys

Forty-nine runs were made on 532.043 g (4.0847 g-atoms) of ordered AuCu. The experimental data are presented in Table IV, and the smooth values, along with the deviations from Kopp's Law expressed as values of ΔCp, are presented in Table V. Figure 9 shows the experimental values, the smoothed selected values, and the Kopp's Law line for the ordered alloy. The ΔCp values are plotted on Figure 10. Cp values were smoothed by drawing a smooth curve on the ΔCp plot and were extrapolated from 20°K to 0°K by extrapolating ΔCp to 0° and then calculating Cp values from the resulting plot. Integration of the smoothed values gave $S^\circ_{298.15} - S^\circ_0 = 9.791$ e.u. and $H^\circ_{298.15} - H^\circ_0 = 1325$ cal/g-atom.

Forty-nine runs were made on 492.393 g (3.7803 g-atoms) of the disordered alloy. Experimental data are in Table IV, smoothed values and ΔCp values are in Table V. The Cp and ΔCp data are shown on

TABLE III. Heat Capacity of the Calorimeter
(Experimental Results)

T, °K	Cp, cal/deg	T, °K	Cp, cal/deg
20.52	0.289	146.07	7.130
22.97	0.368	152.02	7.198
25.57	0.438	156.31	7.271
27.67	0.617	161.97	7.360
30.26	0.781	166.04	7.429
32.30	0.924	172.46	7.544
36.53	1.083	177.84	7.509
40.87	1.565	184.30	7.682
41.05	1.565	197.08	7.940
45.65	1.929	201.49	8.047
50.28	2.336	207.07	8.183
54.69	2.717	213.25	8.243
59.97	3.156	220.68	8.320
64.74	3.532	227.33	8.389
70.15	3.929	236.01	8.433
74.45	4.236	266.55	8.738
78.34	4.489	270.99	8.812
83.32	4.785	273.92	8.837
84.43	4.805	274.49	8.955
90.94	5.187	276.16	9.079
96.82	5.479	277.11	8.881
102.45	5.722	282.35	9.163
108.23	5.994	282.50	9.048
111.95	6.129	284.22	9.346
115.22	6.135	286.89	9.148
120.67	6.438	288.81	9.418
126.22	6.596	290.52	9.305
130.61	6.685	293.14	9.086
136.89	6.839	296.80	9.387

TABLE IV. Experimental Results for AuCu

DISORDERED		ORDERED	
T, °K	Cp, cal/g-atom-deg	T, °K	Cp, cal/g-atom-deg
25.08	0.784	24.66	0.678
26.97	0.921	26.31	0.837
30.22	1.216	28.42	1.025
33.63	1.462	31.43	1.248
40.36	1.898	35.12	1.507
44.06	2.146	40.08	1.719
48.20	2.450	46.73	2.264
52.05	2.672	51.49	2.608
57.49	2.995	55.41	2.843
64.25	3.379	60.20	3.114
69.59	3.619	65.83	3.410
75.40	3.861	71.91	3.652
80.74	4.083	77.75	3.947
85.50	4.249	80.30	3.992
94.65	4.456	84.42	4.179
100.60	4.579	91.84	4.264
106.60	4.695	97.94	4.371
112.75	4.733	103.76	4.643
118.81	4.916	109.77	4.775
124.64	4.982	115.77	4.911
133.05	5.090	122.09	4.951
138.74	5.182	128.30	5.059
144.72	5.247	134.03	5.185
150.92	5.313	140.01	5.279
156.87	5.325	145.94	5.271

TABLE IV. Experimental Results for AuCu (Cont'd.)

DISORDERED		ORDERED	
T, °K	Cp, cal/g-atom-deg	T, °K	Cp, cal/g-atom-deg
162.75	5.357	152.04	5.342
168.79	5.478	157.87	5.379
174.81	5.427	163.88	5.358
181.55	5.487	170.28	5.443
187.10	5.511	176.13	5.503
193.09	5.586	187.92	5.579
197.93	5.538	194.15	5.583
203.94	5.578	199.87	5.633
209.91	5.654	203.94	5.628
216.37	5.653	207.82	5.642
220.05	5.693	212.79	5.663
227.87	5.736	216.75	5.684
233.96	5.751	220.97	5.715
240.08	5.721	233.11	5.765
246.00	5.779	238.85	5.748
251.87	5.775	245.04	5.829
258.02	5.765	251.50	5.825
263.77	5.825	256.14	5.802
269.87	5.849	262.35	5.824
274.46	5.815	268.04	5.831
279.89	5.786	280.18	5.882
285.80	5.889	286.07	5.899
291.52	5.843	292.10	5.905
303.60	5.913	295.98	5.926

TABLE V. Smoothed Values for AuCu

DISORDERED			ORDERED		
T, °K	Cp cal/g-atom-deg	ΔCp	T, °K	$\tilde{Cp}$ cal/g-atom-deg	ΔCp
20	0.496	0.073	20	0.453	0.030
25	0.817	0.078	25	0.779	0.040
30	1.173	0.087	30	1.140	0.054
35	1.535	0.096	35	1.508	0.069
40	1.896	0.092	40	1.854	0.050
45	2.231	0.085	45	2.185	0.039
50	2.554	0.084	50	2.507	0.037
55	2.858	0.088	55	2.815	0.045
60	3.142	0.105	60	3.100	0.063
65	3.413	0.130	65	3.361	0.078
70	3.650	0.145	70	3.600	0.095
75	3.852	0.142	75	3.807	0.097
80	4.030	0.131	80	3.992	0.093
85	4.184	0.115	85	4.158	0.089
90	4.325	0.101	90	4.309	0.085
95	4.455	0.090	95	4.446	0.081
100	4.570	0.080	100	4.566	0.076
110	4.762	0.060	110	4.770	0.068
120	4.927	0.042	120	4.944	0.059
130	5.071	0.025	130	5.090	0.050
140	5.180	0.011	140	5.211	0.042
150	5.276	-0.004	150	5.315	0.035
160	5.356	-0.015	160	5.397	0.026
170	5.424	-0.026	170	5.466	0.016
180	5.485	-0.034	180	5.527	0.008
190	5.540	-0.040	190	5.579	-0.001
200	5.585	-0.045	200	5.620	-0.010
210	5.632	-0.049	210	5.664	-0.017
220	5.673	-0.052	220	5.700	-0.025
230	5.712	-0.054	230	5.735	-0.029
240	5.743	-0.055	240	5.766	-0.032
250	5.774	-0.056	250	5.797	-0.033
260	5.801	-0.055	260	5.825	-0.031
270	5.828	-0.052	270	5.851	-0.029
280	5.854	-0.049	280	5.877	-0.026
290	5.879	-0.046	290	5.902	-0.023
298.15	5.895	-0.044	298.15	5.920	-0.019
300	5.903	-0.042	300	5.929	-0.016

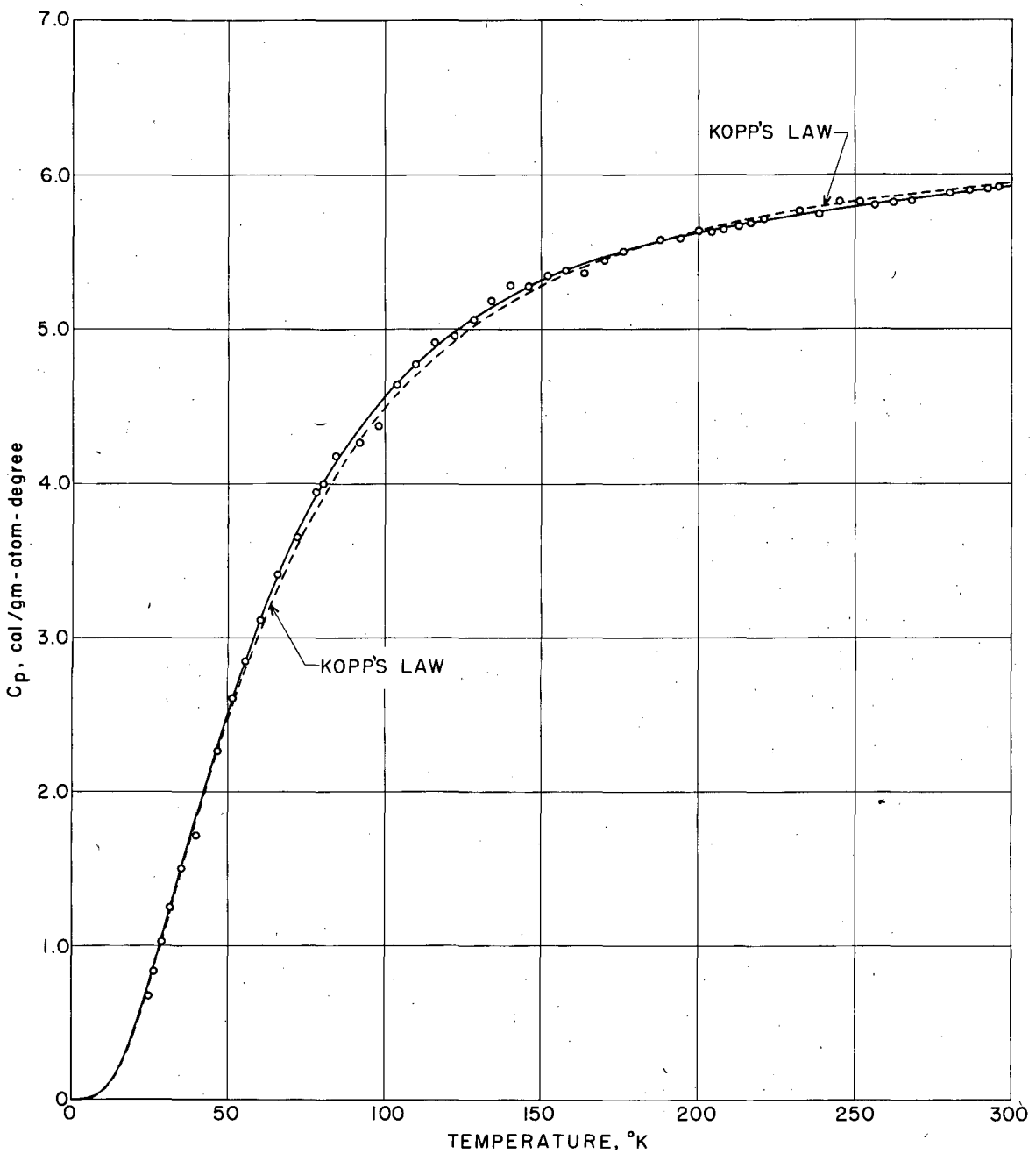

FIGURE 9 HEAT CAPACITY OF ORDERED AuCu.

XBL 6912-6643

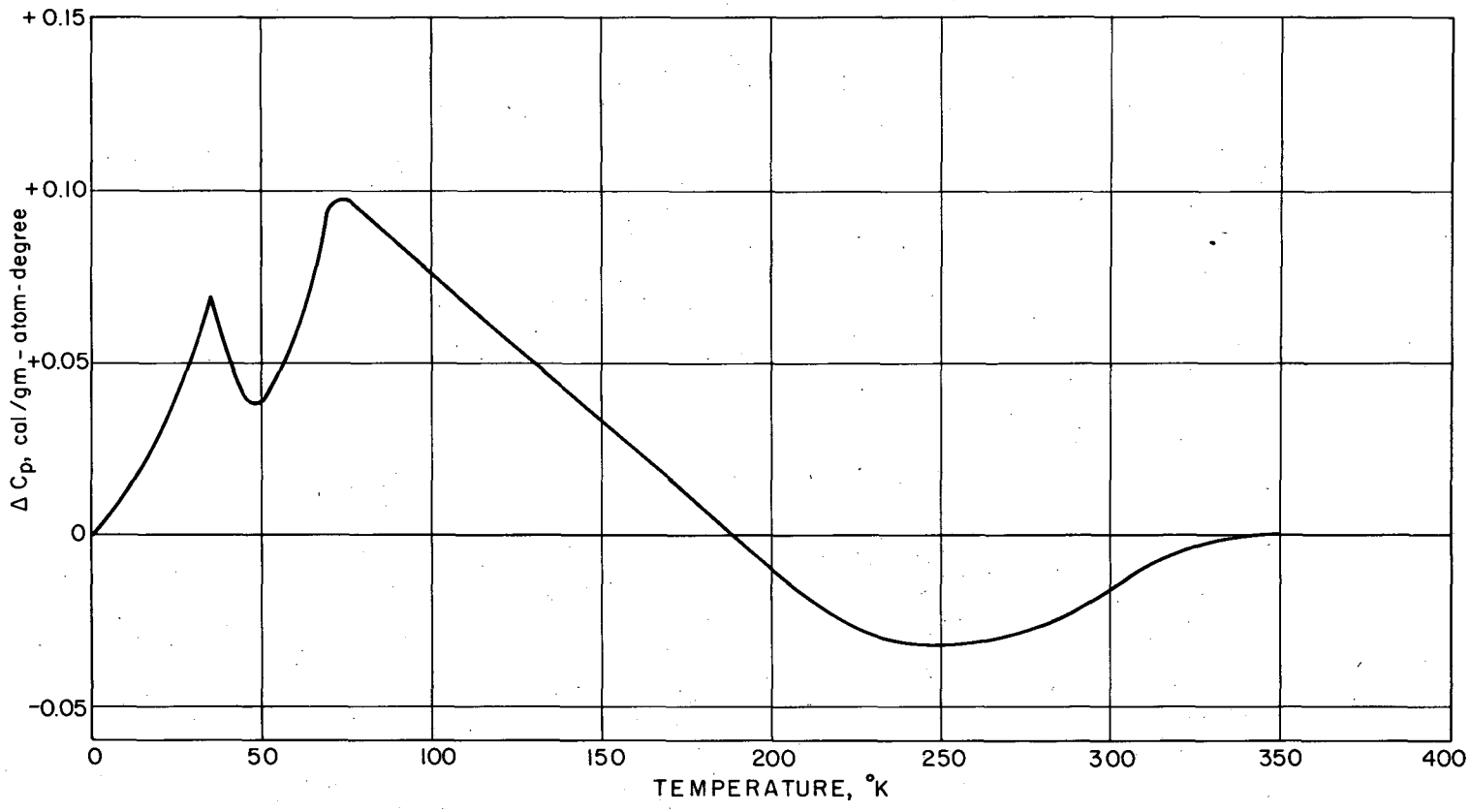

FIGURE 10 DEVIATION FROM KOPP'S LAW FOR ORDERED AuCu.

XBL 6912-6640

Figures 11 and 12, respectively. Extrapolation to 0°K was done in the same manner as for the disordered alloy. Integration of the smooth curve gave $S^\circ_{298.15} - S^\circ_0 = 9.689$ e.u. and $H^\circ_{298.15} - H^\circ_0 = 1323$ cal/g-atom.

Smoothed curves for the ordered state, the disordered state, and for Kopp's Law are plotted on Figure 13 for comparison.

Heats of Formation

Heats of formation of the quenched sample were measured in a tin solution calorimeter in the same manner as Orr,[14] giving the value $\Delta H^\circ_f = -1365(\pm 30)$ cal/g-atom. Orr obtained $\Delta H^\circ_f = -1230$ cal/g-atom for the equilibrium (completely disordered) sample, -1630 cal/g-atom for his quenched sample, and -2150 cal/g-atom for a fully ordered sample. The result for the sample used in this study is only 135 cal/g-atom more exothermic than Orr's value for a fully disordered alloy, showing that the present sample is highly disordered. The sample in the tube which did not break on quenching had $\Delta H^\circ_f = -1530$ cal/g-atom, and thus had considerably more short-range order.

With the aid of high temperature data, ΔS°_0 of disordered AuCu can now be calculated. Combining emf measurements and heat of formation measurements at 800°K[1] yields $\Delta S^\circ_{800} = 1.458$ e.u. Assuming that the disordered alloy obeys Kopp's Law from 800° to 298°K, this same ΔS° value applies at 298°K. One then calculates ΔS°_0 as shown on page 68. A small negative correction must be applied to the value for ΔS°_0 to account for the fact that Kopp's Law is obeyed to

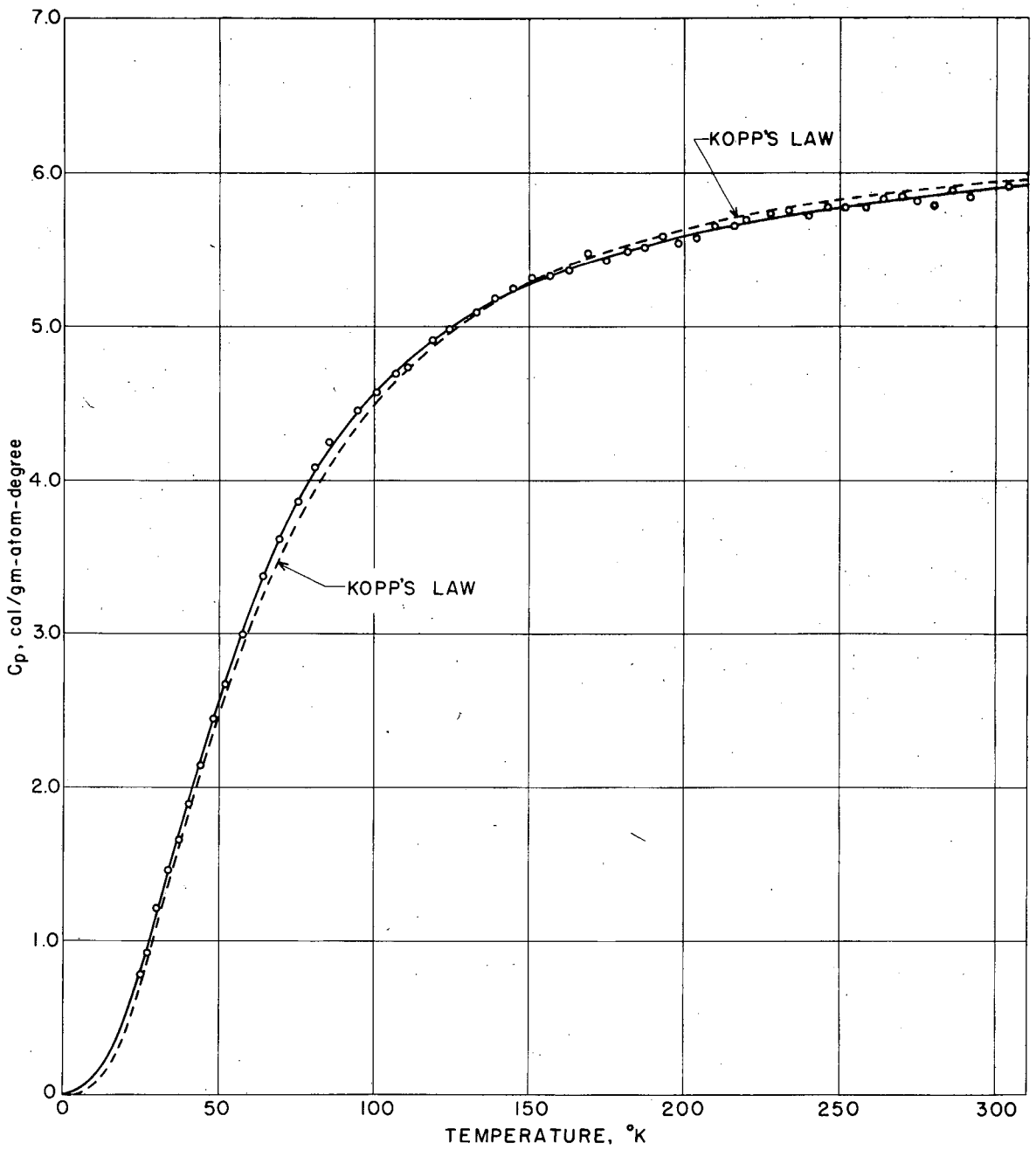

FIGURE 11 HEAT CAPACITY OF DISORDERED AuCu.

XBL 6912-6644

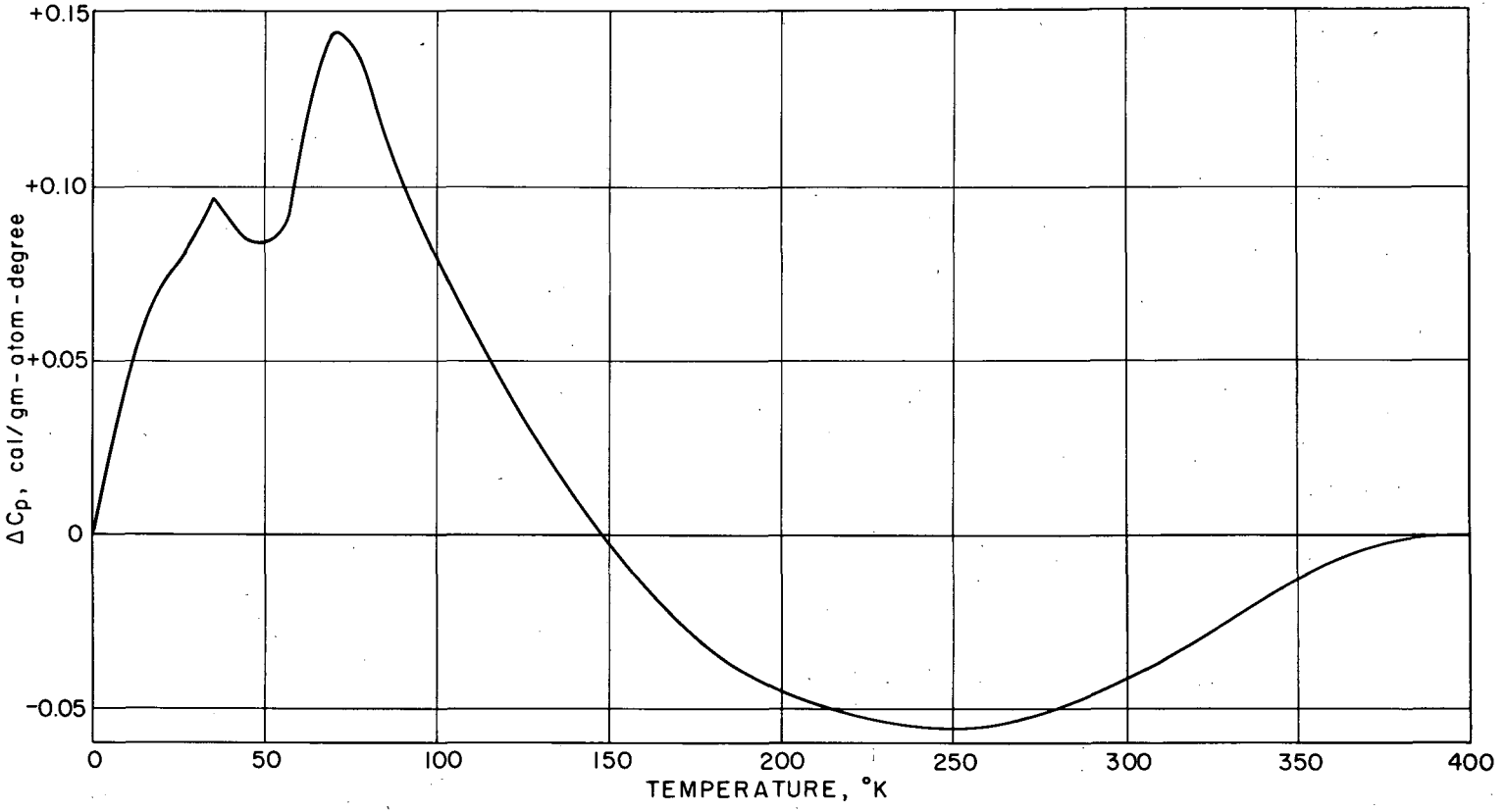

FIGURE 12 DEVIATION FROM KOPP'S LAW FOR DISORDERED AuCu.

XBL 6912-6641

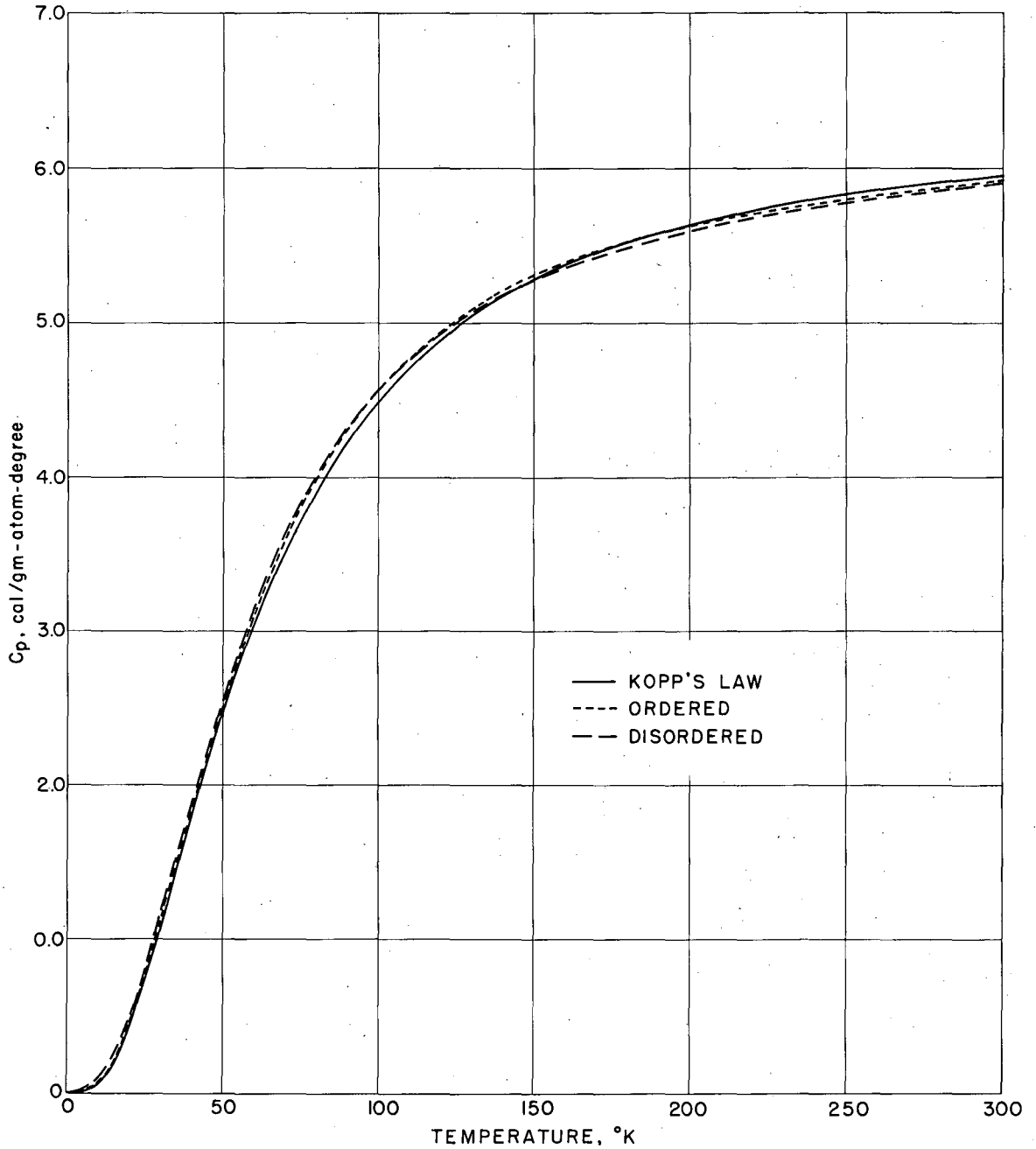

FIGURE 13 HEAT CAPACITY OF ORDERED AND DISORDERED AuCu.

XBL 6912-6645

Calculation of ΔS°_0 for Disordered AuCu

	Reaction		
(1)	$0.5Au_{(298°)} + 0.5Cu_{(298°)} = Au_{0.5}Cu_{0.5(298°,\ disordered)}$	$\Delta S^\circ =$	1.458 e.u.
(2)	$Au_{0.5}Cu_{0.5(298°,\ disordered)} = Au_{0.5}Cu_{0.5(0°,\ disordered)}$	$-(S^\circ_{298}-S^\circ_0) =$	-9.869 e.u.
(3)	$0.5Cu_{(0°)} = 0.5Cu_{(298°)}$	$\frac{1}{2}(S^\circ_{298}-S^\circ_0)_{Cu} =$	3.962 e.u.
(4)	$0.5Au_{(0°)} = 0.5Au_{(298°)}$	$\frac{1}{2}(S^\circ_{298}-S^\circ_0)_{Au} =$	5.676 e.u.
(5)	Correction to disordered AuCu values between 298° and 400°K (see page 64)		-0.005 e.u.
(6)	$0.5Au_{(0°)} + 0.5Cu_{(0°)} = Au_{0.5}Cu_{0.5(0°,\ disordered)}$	$\Delta S^\circ_0 =$	1.222 e.u.

400°K, rather than to 298°K (see Figure 12). This correction amounts to -0.005 e.u., so the true value for ΔS°_0 is 1.222 e.u.

One can also calculate ΔS°_0 from thermal data for the equilibrium state. A plot of ΔH°_f as a function of temperature is given by Orr, Luciat-Labry, and Hultgren.[26] They show a constant value of ΔH°_f from 298° to 523°K, then a sharp, continuous increase from 523° to 683°K, followed by a first-order transformation at 683°K, and then a small increase in ΔH°_f to 800°K, after which the value is constant. The constant regions are an excellent confirmation of the assumption of Kopp's Law at high temperatures. The increase in ΔH°_f below the transformation temperature is attributed to the onset of disordering, while that above the transformation is attributed to the disappearance of short-range order. After making minor adjustments to the curve of Orr, et al., in order to obtain a better fit with all the data, slopes were taken, yielding values of ΔCp. These values were then integrated to give entropies. As shown on the following page, $\Delta S^\circ_{800} = 1.562$ e.u.

If, therefore, the ΔS° value obtained in this manner were used to calculate ΔS°_0 for the disordered state, one would obtain a value for ΔS°_0 which is 0.104 e.u. greater than that previously calculated, i.e., $\Delta S^\circ_0 = 1.332$ e.u. The uncertainty arises from the uncertainties in the high temperature data, and especially in the procedure of taking slopes to obtain Cp values. The error is well within the experimental error of ±0.2 e.u. assigned to the high-temperature emf measurements by

Calculation of ΔS°_0 for Disordered AuCu Using Heat of Formation Data

	Reaction	
(1)	$0.5Au_{(0°)} + 0.5Cu_{(0°)} = Au_{0.5}Cu_{0.5(0°,\ \text{ordered})}$	$\Delta S^\circ_0 = 0.000$ e.u.
(2)	$Au_{0.5}Cu_{0.5(0°,\ \text{ordered})} = Au_{0.5}Cu_{0.5(298°,\ \text{ordered})}$	$(S^\circ_{298} - S^\circ_0) = 9.790$ e.u.
(3)	$Au_{0.5}Cu_{0.5(298°,\ \text{ordered})} = Au_{0.5}Cu_{0.5(683°,\ \text{ordered})}$	$(S^\circ_{683} - S^\circ_{298}) = 5.926$ e.u.
(4)	$Au_{0.5}Cu_{0.5(683°,\ \text{ordered})} = Au_{0.5}Cu_{0.5(683°,\ \text{disordered})}$	$\Delta S^\circ = 0.454$ e.u.
(5)	$Au_{0.5}Cu_{0.5(683°,\ \text{disordered})} = Au_{0.5}Cu_{0.5(800°,\ \text{disordered})}$	$(S^\circ_{800} - S^\circ_{683}) = 1.178$ e.u.
(6)	$0.5Au_{(800°)} = 0.5Au_{(0°)}$	$-\frac{1}{2}(S^\circ_{800} - S^\circ_0) = -8.770$ e.u.
(7)	$0.5Cu_{(800°)} = 0.5Cu_{(0°)}$	$-\frac{1}{2}(S^\circ_{800} - S^\circ_0) = -7.015$ e.u.
(8)	Correction to ordered AuCu values between 298° and 400°K (see page 64)	-0.001 e.u.
(9)	$0.5Au_{(800°)} + 0.5Cu_{(800°)} = Au_{0.5}Cu_{0.5(800°,\ \text{disordered})}$	$\Delta S^\circ_{800} = 1.562$ e.u.
	Experimental value	$\Delta S^\circ_{800} = 1.458$ e.u.
	Difference	0.104 e.u.

Hultgren, et al.[1] The selected value of ΔS°_0 for disordered AuCu was therefore taken to be the average of the two values: 1.280±0.1 e.u. A similar calculation on heats yields ΔH°_0 = 935 cal/g-atom. Combining these results, one can calculate the entropy of disordering at 0°K and also at 298.15°K, viz.:

$$Au_{0.5}Cu_{0.5(ordered)} = Au_{0.5}Cu_{0.5(disordered)} \quad \begin{matrix} \Delta S^\circ_0 = 1.280 \text{ e.u.} \\ \Delta S^\circ_{298.15} = 1.359 \text{ e.u.} \end{matrix}$$

Attempts were made to calculate Gibbs energies of formation for AuCu. The results for the ordered and disordered states are shown in Figure 14. The crossover point is at 760°K, which is 77° above the observed transformation temperature of 683°K. The uncertainty just discussed accounts for this. The value for ΔG° at 800°K is -2390 cal/g-atom, whereas a value of about -2500 cal/g-atom is needed to bring the crossover point into agreement with observations. A shift in the high-temperature entropy of about 10% or 0.1 e.u., would accomplish this.

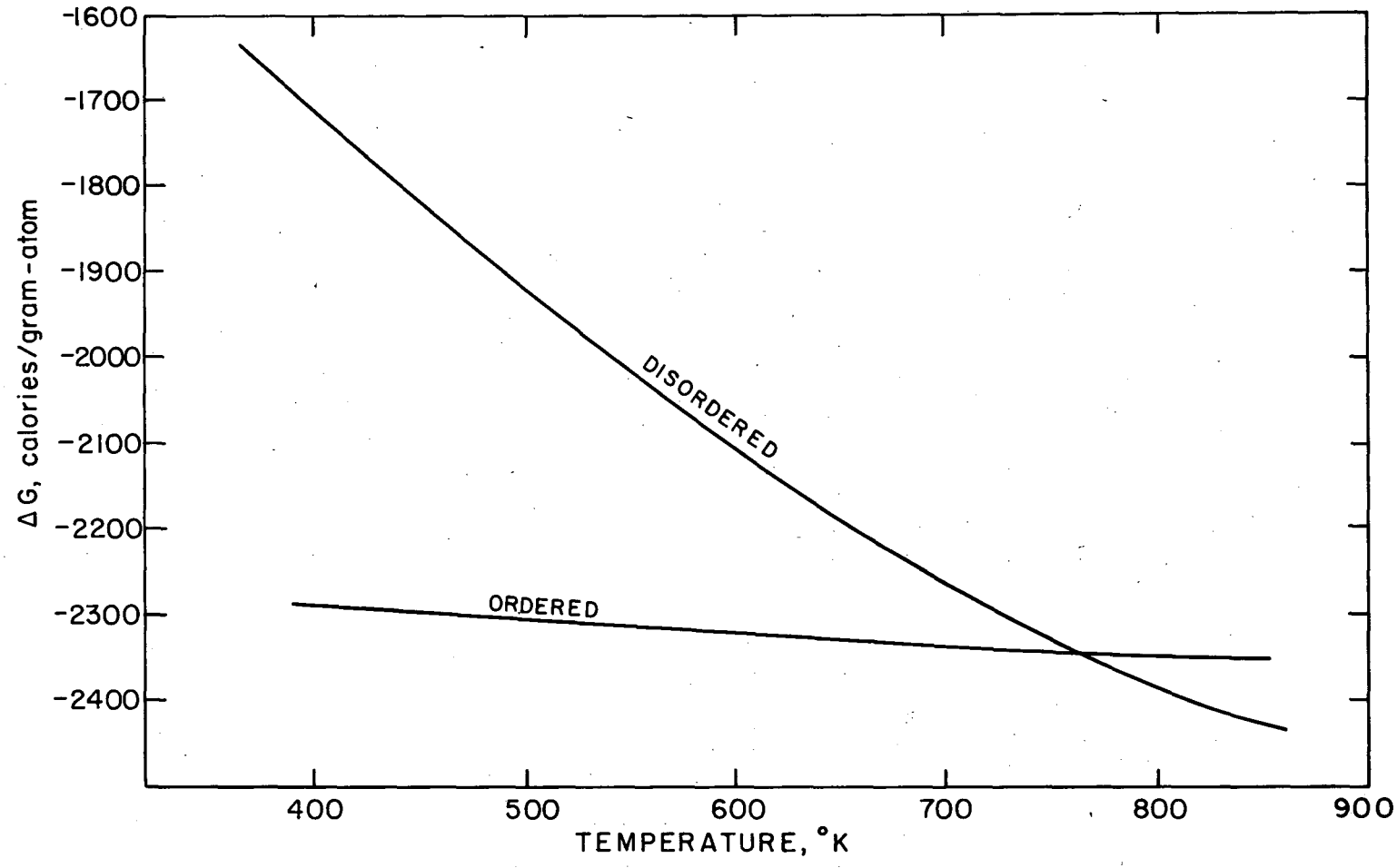

FIGURE 14 CALCULATED GIBBS ENERGY OF ORDERED AND DISORDERED AuCu.

XBL 6912-6639

VII. DISCUSSION AND CONCLUSIONS

The value of ΔS_0° for disordered AuCu, 1.280 e.u., is very near to the theoretical value of R ℓn 2, 1.38 e.u., for a completely disordered (random) 50-50 alloy. That it is somewhat lower than R ℓn 2 e.u. confirms the heat of formation measurements, which show that the sample had a small amount of short-range order. This, of course, was not detectable on the X-ray pattern.

Ordering had little effect on the heat capacities. At low temperatures, Cp of the disordered state is slightly higher than that for the ordered state, while at higher temperatures (above approximately 175°K) Cp of the ordered state is slightly higher. The maximum Cp difference between the two states was less than 0.05 cal/g-atom-deg. One would expect $Cp_{(\text{disordered})}$ to be higher at low temperatures because in a disordered sample there is greater opportunity for low frequency lattice vibrations to occur, thereby lowering the Debye temperature and raising the Cp. Calculations of the apparent Debye temperature, Θ_D, for ordered and disordered AuCu were made, and the results are:

$$\Theta_D(\text{ordered}) = 186°K$$

$$\Theta_D(\text{disordered}) = 165°K,$$

thus confirming these expectations. (In these calculations, the dilation term to Cp was ignored in the absence of the data needed to calculate Cp-Cv.) Previous work on $AuCu_3$ at very low temperatures by

Rayne[27] and Martin[28] also found little effect of ordering on Cp. Other investigations on Ni_3Mn[29] and CuPt[30] found a large effect, but in these systems, magnetic effects may be responsible. (None of these studies extend to temperatures above 4.2°K.) The fact that ordering raises Θ_D is confirmed by all these studies. At higher temperatures, one would also expect Cp of the ordered state to be higher, since, as the critical temperature for disordering is reached, the ordered state releases energy. The crossover of $Cp_{(ordered)}$ over $Cp_{(disordered)}$ at approximately 175°K is not due to the onset of disordering as the temperature is increased. At such low temperatures, diffusion rates are small enough to be negligible. (Heat measurements have shown that disordering does not begin until above 500°K.)

It is noteworthy that the ΔCp curves for the ordered and disordered states have the same general shape. Both have peaks in the neighborhoods of 35° and 75°K, followed by shallow minima near 250°K. The deviations from $\Delta Cp = 0$ are greater for the disordered alloy than for the ordered. The small "valley" near 50°K is deeper for the ordered state than for the disordered. If the "ordered" alloy is assumed to be perfectly ordered, then the depth of this valley could be due to the amount of order in the sample, and it might be presumed to disappear for a perfectly disordered alloy. The fact that the valley is more shallow for the disordered state bears this out. Since some short-range order exists, the disordered lattice is not perfect, and therefore

the lattice vibrations are not uniform throughout the sample. These facts suggest that the ΔCp curve is perhaps smooth and the peaks are perturbations caused by the lack of complete randomness. In order to show this effect more clearly, $Cp_{(disordered)} - Cp_{(ordered)}$ was plotted as a function of temperature. The result, shown in Figure 15, shows the effects of short range order. The dotted portion is an extrapolation of the smooth curve, which would be expected in the case of a completely disordered sample. The effects of the lack of complete order appear as departures from this curve.

Complete disorder is virtually impossible to obtain in massive samples such as were necessary in this study. The quenching method used was chosen so as to be the most rapid possible, but even taking such precautions, some short-range order cannot be prevented. More rapid quenching methods, such as splat cooling, have recently been developed, but only small amounts of material can be produced in this way. A very interesting investigation would be to study the Cp of splat cooled material in which the amount of short-range order is small, or negligible, using a calorimeter designed to accept such small samples. Other work needed to further extend the knowledge of how ordering affects heat capacities would be to study $AuCu_3$ as well as systems with different crystal structures. Results from these studies would be of interest in confirming and extending the present results on AuCu.

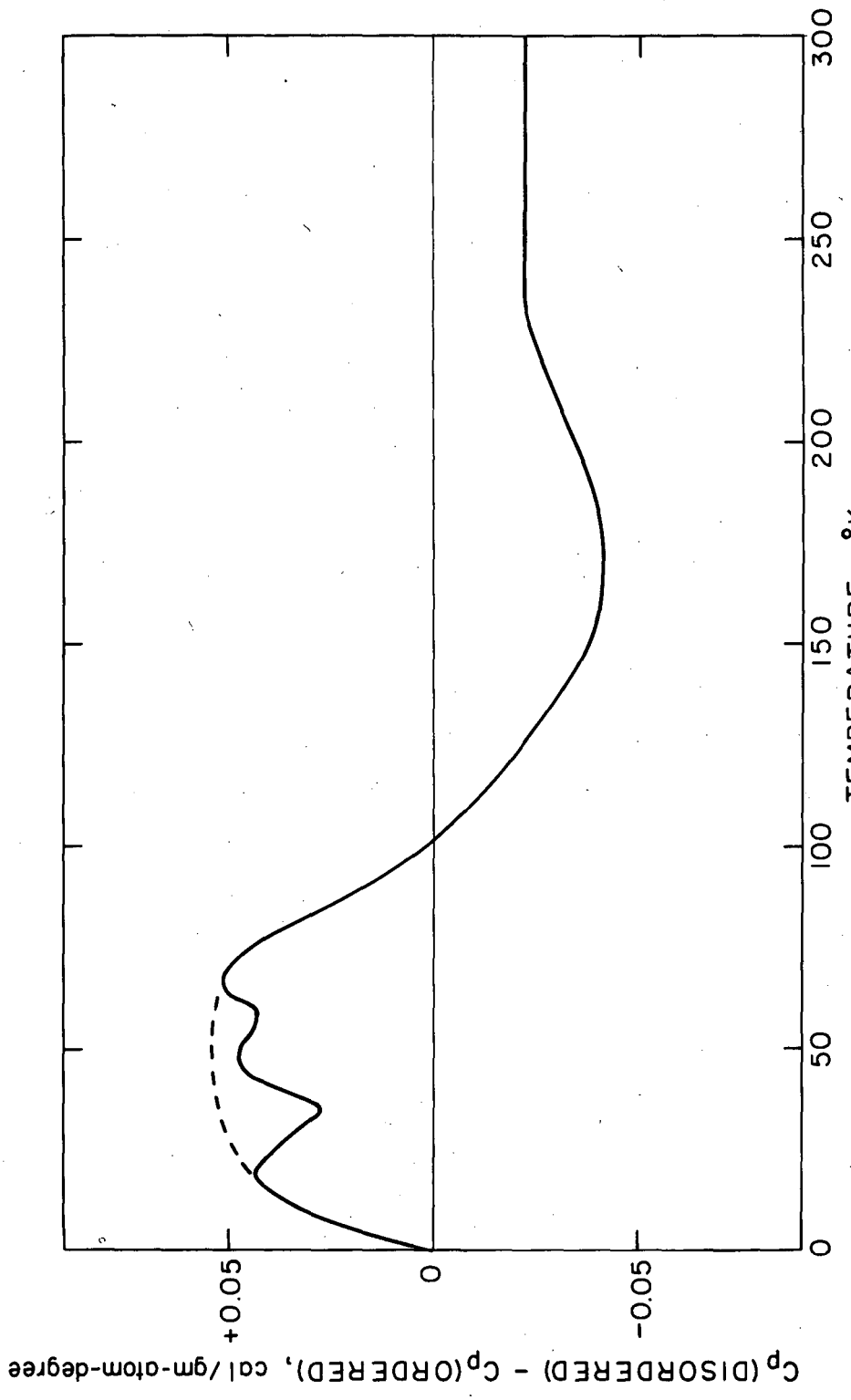

FIGURE .15 HEAT CAPACITY DIFFERENCES FOR Au Cu.

XBL 6912-6638

ACKNOWLEDGEMENTS

I wish to express my gratitude to:

My wife, Patricia, who gave support and encouragement, and who helped in a practical way by sewing the calorimeter thermocouple wires on to their cloth backing strip.

Professor Ralph Hultgren, who has provided much helpful advice and encouragement to me during this project.

Dr. Raymond L. Orr, who has been of help to me during my years as a graduate student.

Mr. Stanley E. Ross, who willingly devoted many hours of his time in assisting in a practical way to all phases of the experimental work. His efforts have contributed a great deal to the successful completion of this project and are greatly appreciated.

Mr. Hong-il Yoon, who also assisted in making some of the measurements.

The staff of the Giauque Low-Temperature Laboratory, who kindly provided the computer program for fitting the resistance-temperature data.

Mrs. Rebecca Palmer, who typed the manuscript.

Mrs. Gloria Pelatowski, who prepared the tracings for the figures.

This work was supported by the U.S. Atomic Energy Commission.

REFERENCES

1. Hultgren, R., R. L. Orr, P. D. Anderson, and K. K. Kelley (1963) Selected Values of Thermodynamic Properties of Metals and Alloys, John Wiley, New York.
2. Hultgren, R., R. L. Orr, and K. K. Kelley (1964-date) Supplement to Selected Values of Thermodynamic Properties of Metals and Alloys. (Loose-leaf sheets issued at irregular intervals.)
3. Dulong, P. L. and A. T. Petit (1819) Ann. chim. phys. 10, 395.
4. Einstein, A. (1907) Ann. Physik 22, 180.
5. Debye, P. (1912) Ann. Physik 39, 789.
6. Kopp, H. (1864) Ann. Chem. Pharm. Suppl. 3, 1, 289.
7. Kelley, K. K., Private communication.
8. Satterthwaite, C. B., R. S. Craig, and W. E. Wallace (1954) J. Am. Chem. Soc. 76, 232.
9. Coffer, L. W., R. S. Craig, C. A. Krier, and W. E. Wallace (1954) J. Am. Chem. Soc. 76, 241.
10. Eastman, E. D. and R. T. Milner (1933) J. Chem. Phys. 1, 444.
11. Hansen, M. (1958) Constitution of Binary Alloys, 2nd Edition, McGraw-Hill, New York.
12. Pearson, W. B. (1967) A Handbook of Lattice Spacings and Structures of Metals and Alloys, Pergammon Press, London.
13. Cullity, B. D. (1956) Elements of X-ray Diffraction, Addison-Wesley, Reading, Mass.

14. Orr, R. L. (1960) Acta Met. 8, 489.

15. Huffstutler, M. C., Jr. (1961) Ph. D. Thesis, University of California, Berkeley.

16. Giauque, W. F. and C. J. Egan (1937) J. Chem. Phys. 5, 45.

17. Gibson, G. E. and W. F. Giauque (1923) J. Am. Chem. Soc. 45, 93.

18. Stout, J. W. (1968) in McCullough, J. P. and D. W. Scott, Ed., Experimental Thermodynamics, Vol. I, Plenum Press, New York.

19. Chelton, D. B. and D. B. Mann (1956) U. S. Atomic Energy Commission Report UCRL-3421.

20. Giauque, W. F., Notes on the Determination of Heat Capacity. Unpublished.

21. International Critical Tables (1930) 1st Ed., 127, 136.

22. Westrum, E. F. (1968) in McCullough, J. P., and D. W. Scott, Ed. Experimental Thermodynamics, Vol. I, Plenum Press, New York.

23. Franzosini, P. (1963) Ric. Sci. Rend. A3, 365.

24. Geballe, T. H. and W. F. Giauque (1952) J. Am. Chem. Soc. 74, 2368.

25. Clusius, K., and P. Harteck (1928) Z. physik. Chem. 134, 243.

26. Orr, R. L., J. Luciat-Labry, and R. Hultgren (1960) Acta. Met. 8, 431.

27. Rayne, J. A. (1957) Phys. Rev. 108, 649.

28. Martin, D. L. (1968) Can. J. Phys. 49, 923.

29. Goldman, J. E. (1953) Rev. Mod. Phys. 25, 108.

30. Roessler, B., and J. A. Rayne (1965) Proc. Low-Temp. Phys., LT9, 1965, 1074.

TECHNICAL INFORMATION DIVISION
LAWRENCE RADIATION LABORATORY
UNIVERSITY OF CALIFORNIA
BERKELEY, CALIFORNIA 94720